pore size and molecular substrate size. In the present study, we used various molecular weight (MW) FITC-dextran molecules as model antigens and assessed the delivery efficiency of FITC-dextran into DCs. (Fig. 1(a–c)). In DCs treated with FITC-dextran (MW 4000) alone, the mean fluorescence intensity was 4-fold higher than non-treated DCs (Fig. 1(a)). On the other hand, upon treatment with FITC-dextran, BLs, and ultrasound, the mean fluorescence intensity was 2-fold higher than that with FITC-dextran alone. We also observed similar phenomena upon treatment with other sizes of FITC-dextran (MW 20,000 and 70,000) (Fig. 1(b), (c)). In addition, to assess the effect of molecular size on delivery efficiency, the fluorescence intensity was compared among FITC-dextrans (MW 4000, 20,000 and 70,000) delivered with BLs and ultrasound (Fig. 1(d)). The percentages of FITC-positive cells (M1 gated) were not affected by molecular weight, determined as 86.0% (MW: 4000), 87.3% (MW: 20,000), and 77.4% (MW: 70,000). On the other hand, the fluorescence intensity decreased as the molecular weight increased. The mean of fluorescence intensities were 24.5 (MW: 4000), 22.4 (MW: 20,000), and 16.5 (MW: 70,000).

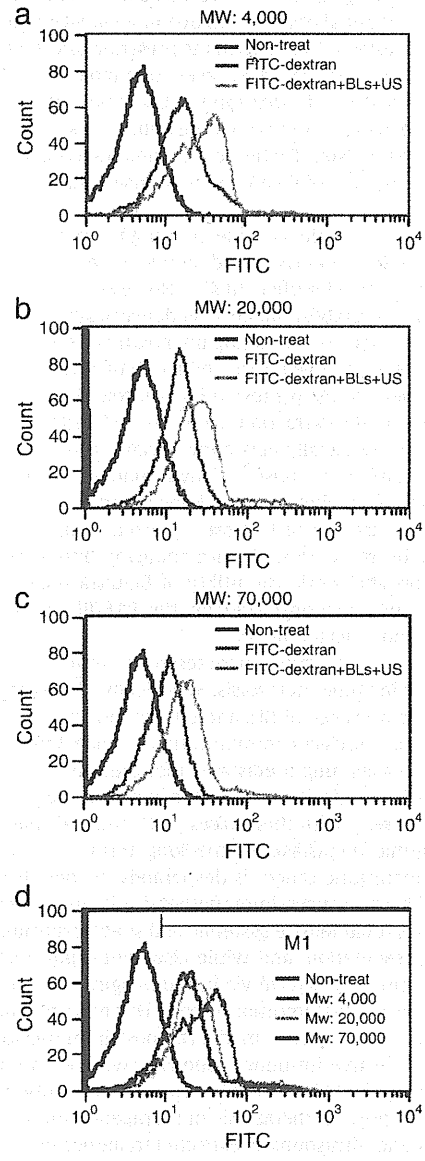

Fig. 1. Effect of molecular size on delivery into DCs using BLs and ultrasound. DCs were incubated with FITC-dextran, exposed to ultrasound in the presence of BLs, and washed with PBS. Delivery efficiency of FITC-dextran was analyzed using flow cytometry. Endocytosis by the DCs was inhibited by the inclusion of 10 mM sodium azide in all solutions and washes. Panels (a) to (c): Experiments were performed with FITC-dextran at a molecular weight of 4000, 20,000, or 70,000, respectively. Panel (d): Molecular weight dependency was analyzed following treatment with the combination of BLs and ultrasound. The percentages of M1 gated cell were quantified as follow: MW: 4000: 86.0%, MW: 20,000: 87.3%, MW: 70,000: 77.4%. The mean of fluorescent intensities were quantified as follow: MW: 4000: 24.5, MW: 20,000: 22.4, MW: 70,000: 16.5.

3.2. B16/BL6-extracted antigen delivery into DCs by BLs and ultrasound

Having demonstrated that the combination of BLs and ultrasound could deliver extracellular molecules of varying sizes, we sought to demonstrate that antigens extracted from B16/BL6 cells could be delivered into DCs by the same technique. Therefore, we assessed the delivery efficiency using Alexa Fluor 633-labeled antigens derived from B16/BL6 cells (Alexa-B16/BL6). As shown in Fig. 2, the DCs treated with antigens or the DCs treated with antigens and either BLs or ultrasound had fluorescence intensity profiles similar to those of untreated DCs. Flow cytometry confirmed this resemblance, with the percentages of Alexa-B16/BL6-positive cells (M2 gated) determined as 5.7% (antigen only), 6.5% (antigen and BLs), and 7.3% (antigen and ultrasound). In contrast, DCs treated with the combination of all three factors (antigens, BLs, and ultrasound) had an elevated fluorescence intensity profile compared with the other groups. Flow cytometry revealed that the percentage of Alexa-B16/BL6-positive cells was 74.1%.

3.3. Reduction in B16/BL6 lung metastasis following immunization with treated DCs

We employed an *in vivo* B16/BL6 experimental lung metastasis model to determine the anti-metastasis efficacy of DCs treated with tumor antigens delivered using BLs and ultrasound. C57BL/6 mice were immunized twice with bone marrow-derived DCs that were either untreated (no antigen exposure) or into which antigens had been delivered by one of four regimens (antigen alone; antigen + BLs; antigen + ultrasound; or antigen + BLs + ultrasound). As shown in Fig. 3(a), immunization with DCs that had been exposed to no antigen, antigen alone, or antigen with BLs *or* ultrasound weakly suppressed tumor metastasis. In contrast, immunization with DCs that had been exposed to antigens delivered via BLs *and* ultrasound reduced lung metastases four-fold, a decrease that was statistically significant ($P<0.05$) compared to the other groups. These numbers were consistent with the results of macroscopic inspection of lungs from the mice by stereoscopic microscopy, as shown in Fig. 3(b).

4. Discussion

The combination of ultrasound and microbubbles/nanobubbles has been reported to be an effective non-viral gene delivery method

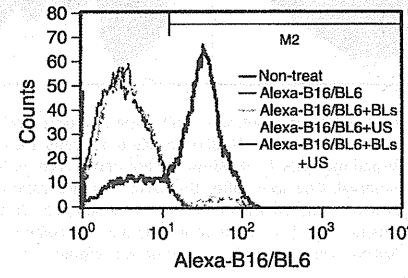

Fig. 2. Intracellular Alexa-B16/BL6 delivery into DCs using BLs and ultrasound. DCs were incubated with Alexa-labeled B16/BL6 extract, exposed (as indicated) to ultrasound and/or BLs, and washed with PBS. Delivery efficiency of Alexa-B16/BL6 was analyzed using flow cytometry. Endocytosis by the DCs was inhibited by the inclusion of 10 mM sodium azide in all solutions and washes. The percentages of M2 gated cell were quantified as follows: Alexa-B16/BL6: 5.7%; Alexa-B16/BL6 + BLs: 6.5%; Alexa-B16/BL6 + ultrasound 7.3%; Alexa-B16/BL6 + BLs + ultrasound: 74.1%.

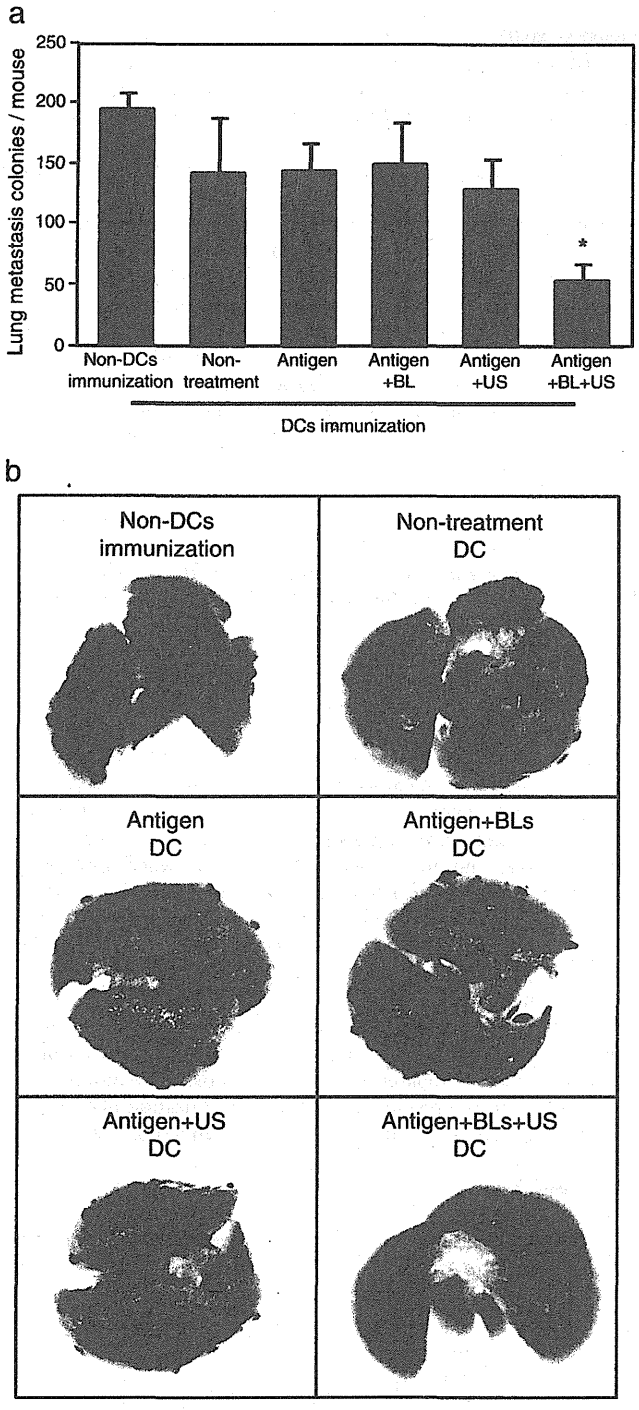

Fig. 3. Reduction of B16/BL6 lung metastasis following immunization with B16/BL6-treated DCs. DCs were treated with B16/BL6-extracted antigens and cultured as described in Materials and methods. C57BL/6 mice were immunized with the DCs twice with a one-week interval. One week after the second immunization, B16/BL6 cells were injected into the tail vein; after another two weeks, animals were sacrificed and lungs assessed for metastases. (a) Counts of lung metastatic colonies (means ± SDs; $n = 6$). *$P < 0.05$ (ANOVA, comparing all DC-immunized groups). (b) Images of lung by stereomicroscope.

for whole cells. This technique also has been applied for peptide and protein delivery [38–40]. In a previous study, we proposed the use of this technique for the delivery of novel antigens into DCs for cancer immunotherapy [29]. Entry into cells is believed to reflect the presence of transient pores in the cell membrane, permitting extracellular molecules direct access to the cytosol [21,28,41]. The present study confirmed that antigen was delivered into DCs by the combination of BLs and ultrasound, with delivery observed despite inhibition of the endocytic pathway. Thus, BLs appear to play a role similar to that of microbubbles for ultrasound-mediated substrate delivery. The present study also demonstrated an inverse correlation between the size of the substrate (MW of FITC-dextran) and the efficiency of delivery (fluorescence intensity). These results are consistent with a dependence of antigen delivery on pore size, which in turn depends on the degree of sonoporated cell membranes by BLs. The effect of pore size is expected to limit the delivery of larger molecules. However, this effect should not prevent the application of BL/ultrasound methods for antigen delivery, given that we were able to demonstrate the immunotherapeutic potential of the technique in an *in vivo* mouse model of lung cancer metastasis. As shown in the present work, we still observed delivery (albeit at a reduced level) even for a molecule (FITC-dextran) with a MW of 70,000. FITC-dextran is a bulky polymer with a straight chain; by comparison, most proteins are tightly packed, with a resulting decrease in apparent size. Therefore, various antigens of a range of sizes should still be able to be delivered into DCs using the BL/ultrasound delivery system.

Melanoma is generally considered a highly immunogenic cancer, and several melanoma-associated antigens (e.g., MAGE, MART-1, gp-100) have been identified [8,42]. However, we thought that it was important to establish an antigen delivery system that was suitable for various extracts containing unknown TAAs, since such a technique would be applicable for the induction of a variety of CTL clones [6]. In the present study, we tested BL/ultrasound delivery with TAAs obtained (via butanol extraction) from B16/BL6 cells. The use of butanol extraction is especially appealing because this method has been shown to solubilize a subset of hydrophobic proteins [33] that would presumably include various known and novel TAAs. Antigens delivered to the cytosol of DCs are expected to induce MHC class I presentation by these DCs, in turn inducing antigen-specific CTLs [12]. In the present work, the utility of BL/ultrasound delivery of a crude extract was demonstrated for the B16/BL6 antigens both *in vitro* (Fig. 2) and *in vivo* (Fig. 3).

The *in vivo* assay described here tested the efficacy of B16/BL6 antigens in reducing lung metastasis. Specifically, DCs were exposed to antigens in the presence of BLs and ultrasound, and the treated cells were used for prophylactic immunization of mice. Immunization significantly decreased lung metastasis, indicating that the treated DCs induced a B16/BL6-specific anti-tumor immune response. Given the poor prognosis seen with metastases [3,4], and the challenge of preventing systemic metastasis in the long term, such a therapeutic strategy for metastatic cancer is desperately needed. From this perspective, DC-based cancer immunotherapy is an attractive option: this approach should induce systemic and specific immune responses via antigen presentation, and while also controlling metastasis and recurrence in the longer term via immunological memory [6]. Matheoud et al. reported that immunization of DCs has a potency to reduce the metastasis in therapeutic model (by post-immunization) [43]. To induce more effective immune responses, we are optimizing about antigen delivery for DCs by BLs/ultrasound. After optimization, we will attempt to prevent metastasis in therapeutic model. The combination of,BLs and ultrasound is expected to induce effective immune response in DC-based cancer immunotherapy by delivering various TAAs into DCs for potential clinical applications.

Acknowledgments

The authors thank Mr. Eisuke Namai, Mr. Yasuyuki Shiono, Mr. Ken Osawa, Ms. Motoka Kawamura, Mr. Ryo Tanakadate, Mr. Kunihiko Matsuo, Mr. Yudai Kawashima, Mr. Hitoshi Uruga, and Ms. Mutsumi Seki (Teikyo University) for their technical assistance,

and Mr. Yasuhiko Hayakawa and Mr. Kosho Suzuki (Nepa Gene Co., Ltd.) for their technical advice regarding ultrasound exposure. This study was supported by the Program for Promotion of Fundamental Studies in Health Sciences of the National Institute of Biomedical Innovation (NIBIO). This work was supported by JSPS KAKENHI (20240053 and 23300192) and Health and Labour Science Research Grants from Ministry of Health, Labour and Welfare.

References

[1] J.W. Gamel, S.L. George, M.J. Edwards, H.F. Seigler, The long-term clinical course of patients with cutaneous melanoma, Cancer 95 (2002) 1286–1293.
[2] C.M. Balch, S.J. Soong, M.B. Atkins, A.C. Buzaid, A. Houghton Jr., J.M. Kirkwood, K.M. McMasters, M.F. Mihm, D.L. Morton, D.S. Reintgen, M.I. Ross, A. Sober, J.A. Thompson, J.F. Thompson, An evidence-based staging system for cutaneous melanoma, CA Cancer J. Clin. 54 (2004) 131–149.
[3] C. Garbe, P. Terheyden, U. Keiholz, O. Kolbl, A. Hauschild, Treatment of melanoma, Dtsch. Arztebl. Int. 105 (2008) 845–851.
[4] U. Vaishampayan, J. Abrams, D. Darrah, V. Joñes, M.S. Mitchell, Active immunotherapy of metastatic melanoma with allogeneic melanoma lysates and interferon, Clin. Cancer Res. 3696 (2002) 3696–3701.
[5] E.M. Levy, M.P. Roberti, J. Mordoh, Natural kiiller cells in human cancer: from biological functions to clinical applications, J. Biomed. Biotechnol. 2011 (2011) 676198.
[6] K. Palucka, H. Ueno, J. Banchereau, Recent developments in cancer vaccines, J. Immunol. 186 (2011) 1325–1331.
[7] P.W. Kantoff, C.S. Higano, N.D. Shore, E.R. Berger, E.J. Small, D.F. Penson, C.H. Redfern, A.C. Ferrari, R. Dreicer, R.B. Sims, Y. Xu, M.W. Frohlich, P.F. Schellhammer, Sipuleucel-T immunotherapy for castration-resistant prostate cancer, N. Engl. J. Med. 363 (2010) 411–422.
[8] S.A. Rosenberg, J.C. Yang, P.F. Robbins, J.R. Wunderlich, P. Hwu, R.M. Sherry, D.J. Schwartzentruber, S.L. Topalian, N.P. Restifo, A. Filie, R. Chang, M.E. Dudley, Cell transfer therapy for cancer: lessons from sequential treatment of a patient with metastatic melanoma, J. Immunother. 26 (2003) 385–393.
[9] P.W. Kantoff, T.J. Schuetz, B.A. Blumenstein, L.M. Glode, D.L. Bilhartz, M. Wyand, K. Manson, D.L. Panicali, R. Laus, J. Schlom, W.L. Dahut, P.M. Arlen, J.L. Gulley, W.R. Godfrey, Overall survival analysis of a phase II randomized controlled trial of a poxviral based PSA-targeted immunotherapy in metastatic castration-resistant prostate cancer, J. Clin. Oncol. 28 (2010) 1099–1105.
[10] F.O. Nestle, A. Farkas, C. Conrad, Dendritic-cell-based therapeutic vaccination against cancer, Curr. Opin. Immunol. 17 (2005) 163–169.
[11] J. Copier, A. Dalgleish, Overview of tumor cell-based vaccines, Int. Rev. Immunol. 25 (2006) 297–319.
[12] R.N. Germain, MHC-dependent antigen processing and peptide presentation: providing ligands for T lymphocyte activation, Cell 76 (1994) 287–299.
[13] P.A. Antony, C.A. Piccirillo, A. Akpinarli, S.E. Finkelstein, P.J. Speiss, D.R. Surman, D.C. Palmer, C.C. Chan, C.A. Klebanoff, W.W. Overwijk, S.A. Rosenberg, N.P. Restifo, CD8+ T cell immunity against a tumor/self-antigen is augmented by CD4+ T helper cells and hindered by naturally occurring T regulatory cells, J. Immunol. 174 (2005) 2591–2601.
[14] P. Elamanchili, M. Diwan, M. Cao, J. Samuel, Characterization of poly(D, L-lactic-co-glycolic acid) based nanoparticulate system for enhanced delivery of antigens to dendritic cells, Vaccine 22 (2004) 2406–2412.
[15] N. Okada, T. Saito, K. Mori, Y. Masunaga, Y. Fujii, J. Fujita, K. Fujimoto, T. Nakanishi, K. Tanaka, S. Nakagawa, T. Mayumi, T. Fujita, A. Yamamoto, Effects of lipofectin-antigen complexes on major histocompatibility complex class I-restricted antigen presentation pathway in murine dendritic cells and on dendritic cell maturation, Biochem. Biophys. Acta 1527 (2001) 97–101.
[16] K. Kawamura, N. Kadowaki, R. Suzuki, S. Udagawa, S. Kasaoka, N. Utoguchi, T. Kitawaki, N. Sugimoto, N. Okada, K. Maruyama, T. Uchiyama, Dendritic cells that endocytosed antigen-containing IgG-liposomes elicit effective antitumor immunity, J. Immunother. 29 (2006) 165–174.
[17] T. Yoshikawa, N. Okada, A. Oda, K. Matsuo, K. Matsuo, Y. Mukai, Y. Yoshioka, T. Akagi, M. Akashi, S. Nakagawa, Development of amphiphilic gamma-PGA-nanoparticle based tumor vaccine: potential of the nanoparticulate cytosolic protein delivery carrier, Biochem. Biophys. Res. Commun. 366 (2008) 408–413.
[18] L. Wang, H. Ikeda, Y. Ikuta, M. Schmitt, Y. Miyahara, Y. Takahashi, X. Gu, Y. Nagata, Y. Sasaki, K. Akiyoshi, J. Sunamoto, H. Nakamura, K. Kuribayashi, H. Shiku, Bone marrow-derived dendritic cells incorporate and process hydrophobized poly-saccaride/oncoprotein complex as antigen presenting cells, Int. J. Oncol. 14 (1999) 695–701.
[19] P. Machy, K. Serre, L. Leserman, Class I-restricted presentation of exogenous antigen acquired by Fcgammareceptor-mediated endocytosis is regulated in dendritic cells, Eur. J. Immunol. 30 (2000) 848–857.
[20] W.J. Greenleaf, M.E. Bolander, G. Sarkar, M.B. Goldring, J.F. Greenleaf, Artificial cavitation nuclei significantly enhance acoustically induced cell transfection, Ultrasound Med. Biol. 24 (1998) 587–595.
[21] Y. Taniyama, K. Tachibana, K. Hiraoka, M. Aoki, S. Yamamoto, K. Matsumoto, T. Nakamura, T. Ogihara, Y. Kaneda, R. Morishita, Development of safe and efficient novel nonviral gene transfer using ultrasound: enhancement of transfection efficiency of naked plasmid DNA in skeletal muscle, Gene Ther. 9 (2002) 372–380.
[22] S. Chen, J.H. Ding, R. Bekeredjian, B.Z. Yang, R.V. Shohet, S.A. Johnston, H.E. Hohmeier, C.B. Newgard, P.A. Grayburn, Efficient gene delivery to pancreatic islets with ultrasonic microbubble destruction technology, Proc. Natl. Acad. Sci. U. S. A. 103 (2006) 8469–8474.
[23] A. Aoi, Y. Watanabe, S. Mori, M. Takahashi, G. Vassaux, T. Kodama, Herpes simplex virus thymidine kinase-mediated suicide gene therapy using nano/microbubbles and ultrasound, Ultrasound Med. Biol. 34 (2008) 425–434.
[24] Z.P. Shen, A.A. Brayman, L. Chen, C.H. Miao, Ultrasound with microbubbles enhances gene expression of plasmid DNA in the liver via intraportal delivery, Gene Ther. 15 (2008) 1147–1155.
[25] S. Sonoda, K. Tachibana, E. Uchino, A. Okubo, M. Yamamoto, K. Sakoda, T. Hisatomi, K.H. Sonoda, Y. Negishi, Y. Izumi, S. Takao, T. Sakamoto, Gene transfer to corneal epithelium and keratocytes mediated by ultrasound with microbubbles, Investig. Ophthalmol. Vis. Sci. 47 (2006) 558–564.
[26] K. Iwanaga, K. Tominaga, K. Yamamoto, M. Habu, H. Maeda, S. Akifusa, T. Tsujisawa, T. Okinaga, J. Fukuda, T. Nishihara, Local delivery system of cytotoxic agents to tumors by focused sonoporation, Cancer Gene Ther. 14 (2007) 354–363.
[27] Y. Taniyama, K. Tachibana, K. Hiraoka, T. Namba, K. Yamasaki, N. Hashiya, M. Aoki, T. Ogihara, K. Yasufumi, R. Morishita, Local delivery of plasmid DNA into rat carotid artery using ultrasound, Circulation 105 (2002) 1233–1239.
[28] R. Suzuki, Y. Oda, N. Utoguchi, K. Maruyama, Progress in the development of ultrasound-mediated gene delivery systems utilizing nano- and microbubbles, J. Control. Release 149 (2011) 36–41.
[29] R. Suzuki, Y. Oda, N. Utoguchi, E. Namai, Y. Taira, N. Okada, N. Kadowaki, T. Kodama, K. Tachibana, K. Maruyama, A novel strategy utilizing ultrasound for antigen delivery in dendritic cell-based cancer immunotherapy, J. Control. Release 133 (2009) 198–205.
[30] K. Inaba, M. Inaba, M. Deguchi, K. Hagi, R. Yasumitsu, S. Ikehara, S. Muramatsu, R.M. Steinman, Granulocytes, macrophages, and dendritic cells arise from a common major histocompatibility complex class II-negative progenitor in mouse bone marrow, Proc. Natl. Acad. Sci. U. S. A. 90 (1993) 3038–3042.
[31] R. Suzuki, T. Takizawa, Y. Negishi, K. Hagisawa, K. Tanaka, K. Tanaka, K. Sawamura, N. Utoguchi, T. Nishioka, K. Maruyama, Gene delivery by the combination of novel liposomal bubbles with perfluoropropane and ultrasound, J. Control. Release 117 (2007) 130–136.
[32] R. Suzuki, T. Takizawa, Y. Negishi, N. Utoguchi, K. Sawamura, K. Tanaka, E. Namai, Y. Oda, Y. Matsumura, K. Maruyama, Tumor specific ultrasound enhanced gene transfer in vivo with novel liposomal bubbles, J. Control. Release 125 (2008) 137–144.
[33] N. Labateya, D.M.P. Thomson, M. Durko, G. Shenouda, L. Robb, R. Scanzano, Extraction of human organ-specific cancer neoantigens from cancer cell and plasma membranes with 1-butanol, Cancer Res. 47 (1987) 1058–1064.
[34] I.A. Ignatovich, E.B. Dizhe, A.V. Pavlotskaya, B.N. Akifiev, S.V. Burov, S.V. Orlov, A.P. Perevozchikov, Complexes of plasmid DNA with basic domain 47–57 of the HIV-1 Tat protein are transferred to mammalian cells by endocytosis-mediated pathways, J. Biol. Chem. 278 (2003) 42625–42636.
[35] K. Sandvig, S. Olsnes, Entry of the toxic proteins abrin, modeccin, ricin, and diphtheria toxin into cells. II. Effect of pH, metabolic inhibitors, and ionophores and evidence for toxin penetration from endocytotic vesicles, J. Biol. Chem. 257 (1982) 7504–7513.
[36] D.A. Zaharoff, J.W. Henshaw, B. Mossop, F. Yuan, Mechanistic analysis of electroporation-induced cellular uptake of macromolecules, Exp. Biol. Med. 233 (2008) 94–105.
[37] J.G. Naglich, M. Jure-Kunkel, E. Gupta, J. Fargnoli, A.J. Henderson, A.C. Lewin, R. Talbott, A. Baxter, J. Bird, R. Savopoulos, R. Wills, R.A. Kramer, P.A. Trail, Inhibition of angiogenesis and metastasis in two murine models by the matrix metalloproteinase inhibitor, BMS-275291, Cancer Res. 61 (2001) 8480–8485.
[38] R. Bekeredjian, S. Chen, P.A. Grayburn, R.V. Shohet, Augmentation of cardiac protein delivery using ultrasound targeted microbubble destruction, Ultrasound Med. Biol. 31 (2005) 687–691.
[39] R. Bekeredjian, H.F. Kuecherer, R.D. Kroll, H.A. Katus, S.E. Hardt, Ultrasound-targeted microbubble destruction augments protein delivery in testes, Urology 69 (2007) 386–389.
[40] M. Kinoshita, K. Hynynen, Intracellular delivery of Bak BH3 peptide by microbubble-enhanced ultrasound, Pharm. Res. 22 (2005) 149–156.
[41] M. Duvshani-Eshet, D. Adam, M. Machluf, The effect of albmin-coated microbubbles in DNA delivery mediated by therapeutic ultrasound, J. Control. Release 112 (2005) 156–166.
[42] P. van der Bruggen, C. Traversari, P. Chomez, C. Lurguin, E. De Plaen, B. Van den Eynde, A. Knuth, T. Boon, A gene encoding an antigen recognized by cytolytic T lymphocytes on a human melanoma, Science 254 (1991) 1643–1647.
[43] D. Matheoud, C. Baey, L. Vimeux, A. Tempez, M. Valente, P. Louche, A.L. Bon, A. Hosmalin, V. Feuillet, Dendritic cells crosspresent antigens from live B16 cells more efficiently than from apoptotic cells and protect from melanoma in a therapeutic model, PLoS One 6 (4) (2011) e19104.

International Journal of Pharmaceutics 422 (2012) 504–509

Contents lists available at SciVerse ScienceDirect

International Journal of Pharmaceutics

journal homepage: www.elsevier.com/locate/ijpharm

Pharmaceutical nanotechnology

Efficient siRNA delivery using novel siRNA-loaded Bubble liposomes and ultrasound

Yoko Endo-Takahashi[a,1], Yoichi Negishi[a,*,1], Yasuharu Kato[a], Ryo Suzuki[b], Kazuo Maruyama[b], Yukihiko Aramaki[a]

[a] Department of Drug Delivery and Biopharmaceutics, School of Pharmacy, Tokyo University of Pharmacy and Life Sciences, Hachioji, Tokyo, Japan
[b] Department of Biopharmaceutics, School of Pharmaceutical Sciences, Teikyo University, Sagamihara, Kanagawa, Japan

ARTICLE INFO

Article history:
Received 8 July 2011
Received in revised form 18 October 2011
Accepted 13 November 2011
Available online 22 November 2011

Keywords:
siRNA delivery
Ultrasound
Bubble liposomes

ABSTRACT

Recently, we developed novel polyethyleneglycol (PEG)-modified liposomes (Bubble liposomes; BLs) entrapping an ultrasound (US) imaging gas and reported that the combination of BLs and US was useful for the delivery of siRNA directly into the cytoplasm. However, the results were obtained using a mixture of BLs and naked siRNA. With systemic injections, it is important to control the biodistribution of both BLs and siRNA. In addition, the delivery of siRNA is affected by nuclease degradation after intravenous administration. In this study, we prepared novel siRNA-loaded BLs (si-BLs) using a cationic lipid, 1,2-dioleoyl-3-trimethylammonium-propane (DOTAP). We demonstrated that siRNA could be loaded onto BLs containing DOTAP and that siRNA-loaded BLs were stable in serum. A specific gene-silencing effect was also achieved by transfection with si-BLs. Thus, the combination of si-BLs with US exposure can be used for delivery of siRNA to a specific tissue via systemic injection.

© 2011 Elsevier B.V. All rights reserved.

1. Introduction

RNA interference (RNAi) has potential application in the development of new therapies for malignant, infectious, and autoimmune diseases. Indeed, synthetic siRNAs are capable of knocking down targets *in vivo* (Frank-Kamenetsky et al., 2008; Halder et al., 2006; Kim et al., 2008; McCaffrey et al., 2002; Morrissey et al., 2005; Niu et al., 2006; Sato et al., 2008; Song et al., 2003; Takeshita et al., 2005; Xia et al., 2007). However, effective and nontoxic delivery is the major challenge to its implementation in a clinical setting.

One novel approach to the administration of a drug or gene is ultrasound (US)-enhanced delivery, which exploits cavitation bubbles produced by the pressure oscillations of US. US pressures above a certain threshold can cause oscillating bubbles to collapse violently, a process known as inertial cavitation. Inertial cavitation is believed to temporarily improve the permeability of cell membranes, enabling the transport of extracellular molecules into viable cells (Delius and Adams, 1999; Duvshani-Eshet and Machluf, 2005; Greenleaf et al., 1998; Holmes et al., 1992; Schratzberger et al., 2002). Furthermore, in combination with microbubbles, contrast agents for medical US imaging improve siRNA transfection efficiency (Du et al., 2011; Kinoshita and Hynynen, 2005; Otani et al., 2009; Tsunoda et al., 2005). However, microbubbles have problems with size, stability, and targeting functionality.

Polyethyleneglycol (PEG)-modified liposomes have excellent biocompatibility, stability, and a long circulation time and can be easily prepared in a variety of sizes and modified to add a targeting function. For these reasons, they are widely used as carriers of drugs, antigens, and genes (Allen et al., 1991; Blume and Cevc, 1990; Harata et al., 2004; Maruyama et al., 1992, 2004). Therefore, PEG-liposomes containing a US imaging gas could be used as novel gene delivery agents. We recently reported that "Bubble liposomes" (BLs) were suitable for gene delivery *in vitro* and *in vivo* (Negishi et al., 2011b,c; Suzuki et al., 2007, 2008a,b). Furthermore, we showed that the combination of BLs and US was also useful for the delivery of siRNA *in vitro* and *in vivo* and that siRNA was introduced directly into the cytoplasm (Negishi et al., 2008). However, the results were obtained using a mixture of BLs and naked siRNA. With systemic injections, transfection efficiency is reduced if the BLs and siRNA are not colocalized in blood vessels. Therefore, it is important to control the biodistribution of both BLs and siRNA. In addition, siRNA is degraded by nuclease and removed rapidly from the circulation after intravenous administration. To overcome these problems, the loading of siRNA onto BLs could be effective for siRNA delivery. Recently, it has been reported that PEGylated lipoplexes (PEG-siPlex) bound to microbubbles led to an increase in the local lipoplex concentration near the cell membrane and resulted in much higher transfection with siRNA in the presence of US (Lentacker et al., 2009; Vandenbroucke et al., 2008). It was also shown that the delivery of siRNA by siRNA-microbubble complexes

* Corresponding author. Tel.: +81 42 676 3183; fax: +81 42 676 3183.
E-mail address: negishi@toyaku.ac.jp (Y. Negishi).
[1] These authors contributed equally to this work.

0378-5173/$ – see front matter © 2011 Elsevier B.V. All rights reserved.
doi:10.1016/j.ijpharm.2011.11.023

was effective for transfection into arteries (Suzuki et al., 2010). However, microbubbles were used in these reports. Microbubbles have problems with size, stability, and targeting functionality as mentioned above. Therefore, we developed nanosized, siRNA-loaded BLs using cholesterol-conjugated siRNA (chol-si-BLs) and demonstrated that using chol-si-BLs led to the stability of siRNA (Negishi et al., 2011a). In this study, we prepared siRNA-loaded BLs (si-BLs) using a cationic lipid. Novel si-BLs were able easily prepared compared with chol-si-BLs. Additionally, this method may have widespread utility for drug delivery systems because it is applicable to various materials possessing negative electrical charges. We also investigated the effects of the amount of PEG in the BLs on their interaction with siRNA, the stability of siRNA in serum, and the gene-silencing effects of transfection with si-BLs and US.

2. Materials and methods

2.1. Cell lines and cultures

COS-7 cells were cultured in Dulbecco's modified Eagle's medium (DMEM; Kohjin Bio Co. Ltd., Tokyo, Japan) supplemented with 10% heat-inactivated fetal bovine serum (FBS; Equitech Bio Inc., Kerrville, TX), 100 units/mL penicillin, and 100 μg/mL streptomycin in a humidified atmosphere containing 5% CO_2 at 37 °C.

2.2. Preparation of liposomes and BLs

To prepare liposomes for conventional BLs, 1,2-dipalmitoyl-sn-glycero-phosphatidylcholine (DPPC) and 1,2-distearoylphosphatidylethanolamine-methoxy-polyethylene glycol (PEG_{2000}) were mixed at a molar ratio of 94:6. Both lipids were purchased from NOF Corporation (Tokyo, Japan). 1,2-dioleoyl-3-trimethylammonium-propane (DOTAP) and 1,2-distearoyl-sn-glycero-3-phosphoethanolamine-N-[methoxy(polyethylene glycol)-750] (PEG_{750}) from Avanti Polar Lipids (Alabaster, AL) were also used. Liposomes with various lipid compositions were prepared by a reverse-phase evaporation method, as described previously (Negishi et al., 2008). In brief, all reagents were dissolved in 1:1 (v/v) chloroform/diisopropylether. Phosphate-buffered saline was added to the lipid solution, and the mixture was sonicated and then evaporated at 47 °C. The organic solvent was completely removed, and the size of the liposomes was adjusted to less than 200 nm using extruding equipment and a sizing filter (Nuclepore Track-Etch Membrane, 200 nm pore size, Whatman plc, UK). After being sized, the liposomes were passed through a sterile 0.45-μm syringe filter (Asahi Techno Glass Co., Chiba, Japan) to sterilize them. The lipid concentration was measured using the Phospholipid C test (Wako Pure Chemical Industries, Ltd., Osaka, Japan). BLs were prepared from liposomes and perfluoropropane gas (Takachiho Chemical Inc., Co., Ltd., Tokyo, Japan). First, 5-mL sterilized vials containing 2 mL of liposome suspension (lipid concentration: 1 mg/mL) were filled with perfluoropropane gas, capped, and then pressurized with 7.5 mL of perfluoropropane gas. The vials were placed in a bath-type sonicator (42 kHz, 100 W, Bransonic 2510J-DTH, Branson Ultrasonics Co., Danbury, CT) for 5 min to form BLs. The zeta potential and mean size of the BLs were determined using the light-scattering method with a zeta potential/particle sizer (Nicomp 380ZLS, Santa Barbara, CA).

2.3. Ultrasound imaging of BLs

BLs diluted with PBS were dispensed into 6-well plates. B-mode recordings were made using a high-frequency ultrasound imaging system (NP60R-UBM, Nepa Gene, Co., Ltd., Chiba, Japan).

2.4. Plasmid DNA and siRNA

The plasmid pCMV-GL3, derived from pGL3-basic (Promega, Madison, WI), is an expression vector encoding the firefly luciferase gene under the control of a cytomegalovirus promoter. Small interfering RNA targeting luciferase (Luciferase GL3 siRNA; siGL3) and a nontargeting siRNA (Control (non-sil.) siRNA; siCont) were purchased from Qiagen K.K. (Tokyo, Japan). Their sequences were as follows: siGL3, *5′-CUUACGCUGAGUACUUCGAdTdT-3′* and *5′-UCGAAGUACUCAGCGUAAGdTdT-3′*; siCont, *5′-UUCUCCGAACGUGUCACGUdTdT-3′* and *5′-ACGUGACACGUUCGGAGAAdTdT-3′*. Nontargeting fluorescein-labeled siRNA (BLOCK-iT Fluorescent Oligo) was purchased from Invitrogen Japan K.K. (Tokyo, Japan).

2.5. Preparation of si-BLs

For the preparation of si-BLs, adequate amounts of siRNA were added to BLs and gently mixed. FITC-labeled siRNA and flow cytometry were used to examine the interaction between siRNA and BLs. The fluorescence intensity of si-BLs was analyzed using a FACSCanto (Becton Dickinson, San Jose, CA). To quantify the amount of siRNA loaded onto the BL surfaces, the BLs were centrifuged at 2000 rpm for 1 min and the unbound siRNA was removed. The BL solution and the aqueous solution containing the unbound siRNA were then boiled for 5 min after which the optical density was measured at 260 nm using a spectrophotometer.

2.6. Stability of siRNA in serum

The BLs, siRNA, and si-BLs were incubated in 50% serum for 15, 30, and 60 min. Serum was used without heat inactivation. The stability of the siRNA was confirmed by 15% polyacrylamide gel electrophoresis. The gel was stained with SYBR SAFE (Invitrogen Japan K.K., Tokyo, Japan) and visualized under ultraviolet light.

2.7. Transfection of siRNA into cells using BLs or si-BLs

The mixture of siRNA (final concentration 100 nM) and BLs or si-BLs (60 μg) in culture medium containing 10% FBS was added to the cells transfected with pDNA on the previous day. The cells were immediately exposed to US (frequency, 2 MHz; duty, 50%; burst rate, 2.0 Hz; intensity 2.0 W/cm^2) for 10 s through a 6-mm diameter probe placed in the well. A Sonopore 3000 (NEPA GENE, Co., Ltd., Chiba, Japan) was used to generate the US. The cells were washed twice with culture medium and cultured for two days.

To measure luciferase activity after transfection, cell lysate was prepared with a lysis buffer (0.1 M Tris–HCl (pH 7.8), 0.1% Triton X-100, and 2 mM EDTA). Luciferase activity was measured using a luciferase assay system (Promega, Madison, WI) and a luminometer (LB96 V, Belthold Japan Co., Ltd., Tokyo, Japan). The activity is reported in as relative light units (RLU) per mg of protein.

2.8. Statistical analyses

All data are reported as the mean ± SD ($n = 4$). Data were considered significant when $P < 0.05$. The t-test was used to calculate statistical significance.

3. Results

3.1. Preparation of BLs containing DOTAP

Initial experiments were performed to investigate whether liposomes containing a cationic lipid, DOTAP, could entrap a US imaging gas as well as conventional BLs. We prepared liposomes containing DOTAP in various amounts and attempted to entrap the gas. The

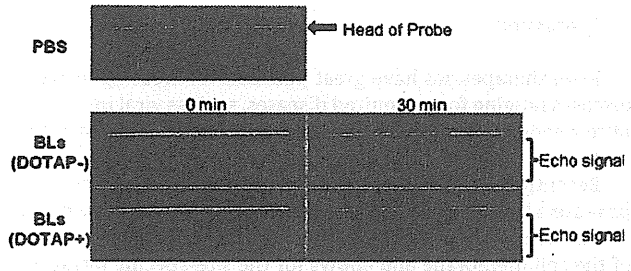

Fig. 1. Ultrasonographic images of a plate containing BLs with or without DOTAP.

liposomes containing up to 15 mol% DOTAP became cloudy, and we concluded that they could effectively entrap the imaging gas (data not shown). The liposomes containing more than 15 mol% DOTAP had difficulty entrapping the gas. We also examined BLs containing DOTAP using a high-frequency US imaging system. The system is a two-dimensional US image display composed of bright dots representing the US echoes. The brightness of each dot is determined by the amplitude of the returned echo signal. As shown in Fig. 1, the US echo signal was detected even 30 min later.

3.2. Effects of polyethyleneglycol on the interaction of siRNA with BLs

To assess whether siRNA could be loaded onto the surface of BLs, we used a fluorescence-activated cell sorter, the FACSCanto. We also prepared BLs containing different lengths of PEG to assess the effect of PEG on BL interactions with siRNA. As shown in Fig. 2, BLs not containing DOTAP were successfully loaded with siRNA. Approximately 40% of the BLs were FITC positive. Approximately 45% of the BLs containing DOTAP but not containing PEG_{750} were FITC positive. In contrast, BLs containing DOTAP and PEG_{750} were more heavily loaded with siRNA. Approximately 80% were FITC positive. Thus, in all subsequent experiments, BLs composed of DPPC, DOTAP, PEG_{2000}, and PEG_{750} (in a 79:15:3:3 molar ratio) were used.

Table 1
Size (nm) and zeta potential (mV) of BLs and si-BLs.

Lipid composition of BLs (molar ratio)	BLs	si-BLs
DPPC:PEG_{2000} = 94:6	528.3 nm	587.9 nm
DPPC:DOTAP:PEG_{2000}:PEG_{750} = 79:15:3:3	749.0 nm	862.2 nm
DPPC:PEG_{2000} = 94:6	−0.81 mV	−0.42 mV
DPPC:DOTAP:PEG_{2000}:PEG_{750} = 79:15:3:3	−0.20 mV	−0.13 mV

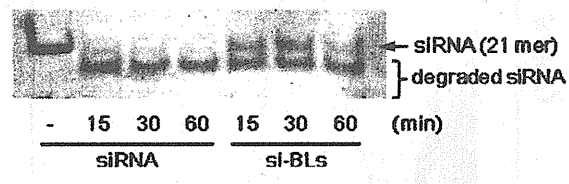

Fig. 3. Stability of siRNA in the presence of serum. Naked siRNA or si-BLs (DOTAP (+), PEG_{2000} and PEG_{750} (3:3)) were subjected to 50% serum degradation at 37 °C for 0.5 or 1 h and confirmed by 15% acrylamide gel electrophoresis.

As shown in Table 1, there was almost no change in the size and zeta potential of the BLs after siRNA was added.

We investigated the stability of siRNA in serum. Small interfering RNA held by BLs showed increased stability in 50% serum compared with free siRNA, although some siRNA was degraded (Fig. 3). We also examined the change in the amount of siRNA bound to BLs when the concentration of the siRNA was increased. As shown in Fig. 4, the amount siRNA loaded increased in a dose-dependent manner. We finally estimated that 60 μg of BLs could be loaded with at least 100 pmol of siRNA and that approximately 30% of the siRNA was bound to the lipid surface.

3.3. Transfection of siRNA into cells using BLs or si-BLs

Before the transfection experiments, we investigated the destruction efficiency of si-BLs under the US exposure. The solution of si-BLs was exposed to the same conditions used for *in vitro* transfection and was analyzed using the FACSCanto. Unlike the solution of si-BLs before US exposure, no fluorescence was detected in the

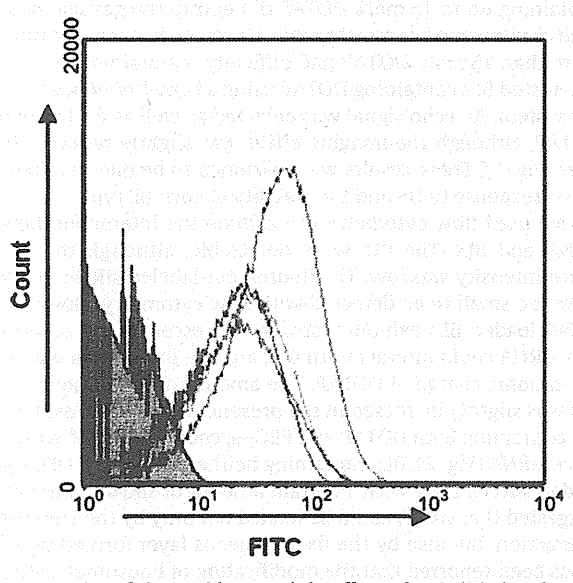

Fig. 2. Interaction of siRNA with BLs and the effects of PEG chain length on the interaction. The interaction was examined by analyzing a mixture of FITC-siRNA (50 pmol) and various BLs (60 μg) with the FACSCanto; gray area: BLs only; red curve: si-BLs (DOTAP (−), PEG_{2000} and PEG_{750} (molar ratio, 6:0)); green curve: si-BLs (DOTAP (+), PEG_{2000} and PEG_{750} (6:0)); blue curve: si-BLs (DOTAP (−), PEG_{2000} and PEG_{750} (3:3)); purple curve: si-BLs (DOTAP (+), PEG_{2000} and PEG_{750} (3:3)).

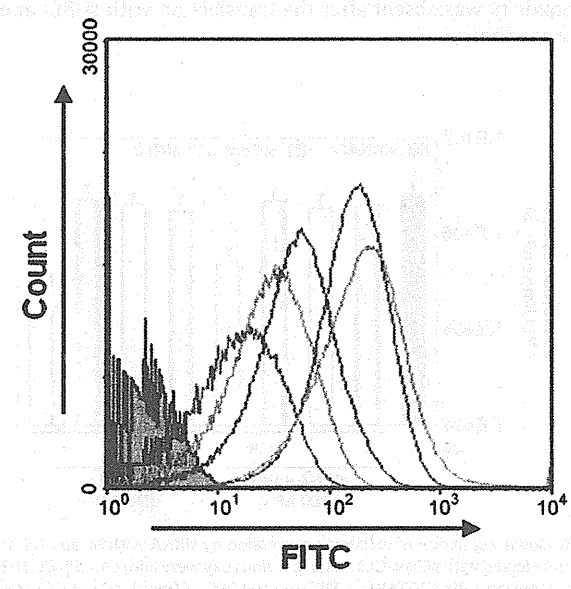

Fig. 4. Loading of siRNA onto BLs. The interaction was examined by analyzing a mixture of FITC-siRNA (12.5–200 pmol) and BLs (60 μg) containing DPPC, DOTAP, PEG_{2000} and PEG_{750} (79:15:3:3) with FACSCanto; gray area: BLs only; red curve: si-BLs (siRNA 12.5 pmol); green curve: si-BLs (siRNA 25 pmol); blue curve: si-BLs (siRNA 50 pmol); purple curve: s si-BLs (siRNA 100 pmol); light blue curve: si-BLs (siRNA 200 pmol).

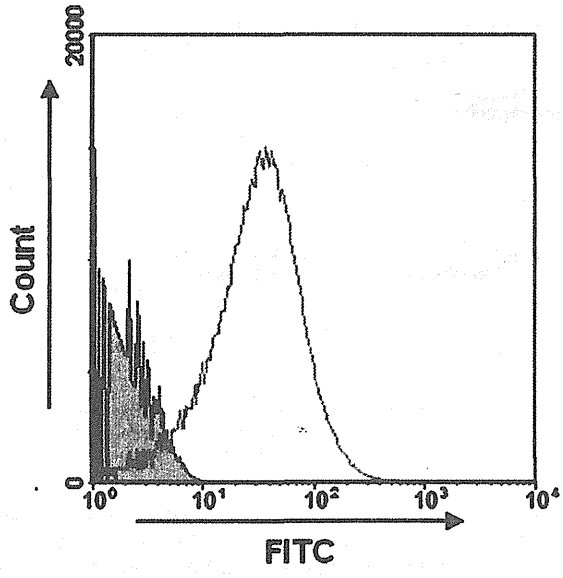

Fig. 5. Effects of US on si-BLs. The interaction was examined by analyzing a mixture of FITC-siRNA (50 pmol) and BLs (60 μg) containing DPPC, DOTAP, PEG_{2000}, and PEG_{750} (79:15:3:3) with the FACSCanto; gray area: BLs only; red curve: si-BLs; green curve: solution of si-BLs after US exposure (frequency, 2 MHz; duty, 50%; burst rate, 2.0 Hz; intensity, 2.0 W/cm^2; time, 10 s). (For interpretation of the references to color in this figure legend, the reader is referred to the web version of the article.)

solution (Fig. 5). This result suggested that the US caused the release of siRNA from the surface of the BLs.

To investigate the gene-silencing effects of siRNA transfection with si-BLs and US, cells transfected with pDNA encoding firefly luciferase (pCMV-GL3) on the previous day were added to BLs loaded with nontargeting control or luciferase-targeting siRNA (siCont or siGL3) and exposed to US (Fig. 6). Approximately 80% of luciferase expression was specifically blocked by siGL3 in the si-BLs-treated group and in the group treated with conventional BLs. Cytotoxicity was absent after the transfection with si-BLs and US (data not shown).

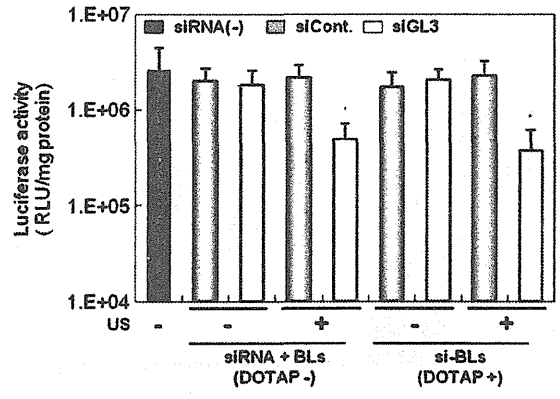

Fig. 6. Down-regulation of luciferase expression by siRNA with BL and US. COS-7 cells transfected with pCMV-GL3 on the previous day were added to siRNA (100 nM) and conventional BLs (DOTAP (−), PEG_{2000}, and PEG_{750} (molar ratio, 6:0)) or si-BLs (DOTAP (+), PEG_{2000}, and PEG_{750} (molar ratio, 3:3)) and applied. At 2 days posttransfection, luciferase expression was measured. siRNA(−); the group not transfected with siRNA, siCont; the group transfected with nontargeting siRNA (siCont), siGL3; the group transfected with siRNA targeting luciferase (siGL3). *P values <0.05 compared with the group transfected with siCont. All data are reported as the mean ± SD (n=4).

4. Discussion

RNAi therapeutics have great potential for treating intractable diseases ranging from acquired diseases, such as viral infections, to purely genetic disorders. However, inefficient delivery into specific organs has hindered their clinical application.

Recently, a combination of microbubbles and US has been proposed as a less invasive and tissue-specific method of gene delivery. The combination produces transient changes in the permeability of the cell membrane and allows for the site-specific intracellular delivery of molecules such as dextran, pDNA, peptides, and siRNA both *in vitro* and *in vivo* (Du et al., 2011; Kinoshita and Hynynen, 2005; Li et al., 2003; Otani et al., 2009; Sonoda et al., 2006; Taniyama et al., 2002a,b; Tsunoda et al., 2005; Unger et al., 2004). However, because existing microbubbles have problems with size, stability, and targeting functionality, we developed liposomal bubbles (BLs). BLs are an effective and novel tool for gene and siRNA delivery *in vitro* and *in vivo* (Negishi et al., 2008, 2011b,c; Suzuki et al., 2007, 2008a,b). Our method using BLs and US did not involve endocytosis, and siRNA was directly introduced into the cytoplasm within a fairly short time. Thus, it seems unnecessary to consider the escape of siRNA from the endosome and the degradation of siRNA in lysosomes, although the endosomal escape is an important issue in other delivery tools. Furthermore transfection methods using physical energy other than US are expected and are currently being developed (Endoh and Ohtsuki, 2009; Kong et al., 2004; Oliveira et al., 2007; Schiffelers et al., 2005; Takei et al., 2008). These methods are difficult to apply to deep tissue. In contrast, US is able to control the accessible tissue sites by changing of the frequency and to reach the deep tissues. However, our previous results were obtained using a mixture of BLs and naked siRNA, which do not colocalize in blood vessels after intravenous administration. Additionally, siRNA is susceptible to degradation by nucleases and rapid removal from circulation. Consequently, these factors may cause a reduction in transfection efficiency. In this study, we prepared siRNA-loaded BLs (si-BLs) using a cationic lipid as a more effective, efficient delivery tool for systemic injections.

We initially attempted to entrap a US imaging gas in BLs containing DOTAP, a cationic lipid often used for gene delivery. Liposomes containing up to 15 mol% DOTAP did entrap the gas and could be used as ultrasound contrast agents. However, liposomes containing more than 15 mol% DOTAP had difficulty maintaining the gas. We also tested BLs containing DOTAP using a high-frequency US imaging system. An echo signal was detected as well as for BLs without DOTAP, although the imaging effect was slightly reduced 30 min later (Fig. 1). These results were assumed to be due to differences in the response to US and the stability of each BL type.

We used flow cytometry to examine the interaction between siRNA and BLs. The BLs were detectable, although the fluorescence intensity was low. The fluorescein-labeled siRNA molecules were too small to be detected with flow cytometry. However, the siRNA-loaded BLs exhibited strong fluorescence. We determined that siRNA could interact with BLs, and the interaction was due to the cationic charge of DOTAP. The amount of siRNA bound to the BLs was slightly increased in the presence of DOTAP. Furthermore, BLs containing both DOTAP and PEG_{750} could be loaded with much more siRNA (Fig. 2). BLs containing neither DOTAP nor PEG_{750} also loaded successfully with a certain amount of siRNA. These results suggested that siRNA could be loaded not only by the electrostatic interaction, but also by the fixed aqueous layer formed with PEG. It has been reported that the modification of liposomes with short and long PEG chains increases the fixed aqueous layer thickness (Sadzuka et al., 2002). We considered that the structural changes in the PEG chain facilitated interaction between the cationic lipid and anionic siRNA. Moreover, there were no significant changes in size after adding siRNA (Table 1). The data suggested that siRNA

was bound to the surface of BLs and that BLs did not aggregate. We also investigated the stability of siRNA interacting with BLs in 50% serum. Although some siRNA was degraded, siRNA held by BLs showed increased stability in 50% serum compared with free siRNA (Fig. 3). In the solution of si-BLs, free siRNA was present with si-BLs. Therefore, the siRNA not held by BLs was degraded. We examined the change in the amount of bound siRNA by adding various amounts of siRNA to BLs. As shown in Fig. 4, the amount of siRNA loaded onto BLs (60 μg) increased with siRNA addition in a dose-dependent manner up to 100 pmol.

We also investigated the effects of US exposure on si-BLs by analyzing the si-BL solution after exposure under the same conditions used for the *in vitro* transfection. No fluorescence was detected. Moreover, there were only a few detectable molecules in the solution of si-BLs after US exposure, and the histogram representing the results was almost parallel to the horizontal axis, similar to the solution of free siRNA (Fig. 5). This result suggested that US exposure collapsed si-BLs, releasing siRNA from the surface of the BLs. We confirmed that there was no damage to siRNA from US exposure by electrophoresis (data not shown). Undetectable fluorescence does not necessarily mean that siRNA were released from BLs: it is also possible that siRNA interacted with lipids or BLs that reverted to liposomes by degassing. However, the gene-silencing effects of siRNA transfection via si-BLs and US were comparable to those of siRNA transfection with conventional BLs and US (Fig. 6). Therefore, it appears that the exposure to US-induced cavitation, the release of siRNA from BLs, and the delivery of siRNA into the cytoplasm. We are currently developing BLs composed of lipids other than DPPC or DOTAP in attempts to form more stable and effective BLs. In the future, we will also examine siRNA delivery and disease-associated gene-silencing effects.

The preparation method of si-BLs developed in this study was easier than that of chol-si-BLs reported previously (Negishi et al., 2011a). Furthermore, BLs containing cationic lipid are expected to have widespread application to delivery tools of various molecules possessing negative electric charges. We confirmed that not only siRNA but also pDNA can be loaded onto BLs (p-BLs). Additionally, microbubbles conjugated to an antibody and having a targeting function have been developed recently (Behm et al., 2008; Leong-Poi et al., 2005; Palmowski et al., 2008). Liposomes can be easily modified to add a targeting function. Thus, the development of targeting si-BLs or p-BLs using an antibody or peptide is expected to lead to beneficial clinical applications for various diseases.

5. Conclusion

In this study, we showed that si-BLs could deliver siRNA as well as conventional BLs, although there remains room for improvement. Additionally, BLs containing a cationic lipid interacted with siRNA and protected the siRNA against nuclease degradation. These results suggest that si-BLs combined with US exposure may be useful for delivering siRNA to a tissue or organ via systemic injection.

Acknowledgements

We are grateful to Dr. Katsuro Tachibana (Department of Anatomy, School of Medicine, Fukuoka University) for technical advice regarding the induction of cavitation with US, to Ms. Yuko Ishii and Ms. Arisa Nakamura (School of Pharmacy, Tokyo University of Pharmacy and Life Sciences) for excellent technical assistance, and to Mr. Yasuhiko Hayakawa and Mr. Kosho Suzuki (Nepa Gege Co., Ltd.) for technical advice regarding US exposure. This study was supported by a Grant for Industrial Technology Research (04A05010) from the New Energy and Industrial Technology Development Organization (NEDO) of Japan, a Grant-in-Aid for Exploratory Research (18650146) from the Japan Society for the Promotion of Science, a Grant-in-Aid for Scientific Research (B) (20300179) from the Japan Society for the Promotion of Science, and a Grant-in-Aid for Young Scientists (B) (21790164) from the Japan Society for the Promotion of Science.

References

Allen, T.M., Hansen, C., Martin, F., Redemann, C., Yau-Young, A., 1991. Liposomes containing synthetic lipid derivatives of poly(ethylene glycol) show prolonged circulation half-lives in vivo. Biochim. Biophys. Acta 1066, 29–36.

Behm, C.Z., Kaufmann, B.A., Carr, C., Lankford, M., Sanders, J.M., Rose, C.E., Kaul, S., Lindner, J.R., 2008. Molecular imaging of endothelial vascular cell adhesion molecule-1 expression and inflammatory cell recruitment during vasculogenesis and ischemia-mediated arteriogenesis. Circulation 117, 2902–2911.

Blume, G., Cevc, G., 1990. Liposomes for the sustained drug release in vivo. Biochim. Biophys. Acta 1029, 91–97.

Delius, M., Adams, G., 1999. Shock wave permeabilization with ribosome inactivating proteins: a new approach to tumor therapy. Cancer Res. 59, 5227–5232.

Du, J., Shi, Q.S., Sun, Y., Liu, P.F., Zhu, M.J., Du, L.F., Duan, Y.R., 2011. Enhanced delivery of monomethoxypoly(ethylene glycol)-poly(lactic-co-glycolic acid)-poly l-lysine nanoparticles loading platelet-derived growth factor BB small interfering RNA by ultrasound and/or microbubbles to rat retinal pigment epithelium cells. J. Gene Med. 13, 312–323.

Duvshani-Eshet, M., Machluf, M., 2005. Therapeutic ultrasound optimization for gene delivery: a key factor achieving nuclear DNA localization. J. Control. Release 108, 513–528.

Endoh, T., Ohtsuki, T., 2009. Cellular siRNA delivery using cell-penetrating peptides modified for endosomal escape. Adv. Drug Deliv. Rev. 61, 704–709.

Frank-Kamenetsky, M., Grefhorst, A., Anderson, N.N., Racie, T.S., Bramlage, B., Akinc, A., Butler, D., Charisse, K., Dorkin, R., Fan, Y., Gamba-Vitalo, C., Hadwiger, P., Jayaraman, M., John, M., Jayaprakash, K.N., Maier, M., Nechev, L., Rajeev, K.G., Read, T., Röhl, I., Soutschek, J., Tan, P., Wong, J., Wang, G., Zimmermann, T., de Fougerolles, A., Vornlocher, H.P., Langer, R., Anderson, D.G., Manoharan, M., Koteliansky, V., Horton, J.D., Fitzgerald, K., 2008. Therapeutic RNAi targeting PCSK9 acutely lowers plasma cholesterol in rodents and LDL cholesterol in nonhuman primates. Proc. Natl. Acad. Sci. U.S.A. 105, 11915–11920.

Greenleaf, W.J., Bolander, M.E., Sarkar, G., Goldring, M.B., Greenleaf, J.F., 1998. Artificial cavitation nuclei significantly enhance acoustically induced cell transfection. Ultrasound Med. Biol. 24, 587–595.

Halder, J., Kamat, A.A., Landen, C.N., Han, L.Y., Lutgendorf, S.K., Lin, Y.G., Merritt, W.M., Jennings, N.B., Chavez-Reyes, A., Coleman, R.L., Gershenson, D.M., Schmandt, R., Cole, S.W., Lopez-Berestein, G., Sood, A.K., 2006. Focal adhesion kinase targeting using *in vivo* short interfering RNA delivery in neutral liposomes for ovarian carcinoma therapy. Clin Cancer Res. 12, 4916–4924.

Harata, M., Soda, Y., Tani, K., Ooi, J., Takizawa, T., Chen, M., Bai, Y., Izawa, K., Kobayashi, S., Tomonari, A., Nagamura, F., Takahashi, S., Uchimaru, K., Iseki, T., Tsuji, T., Takahashi, T.A., Sugita, K., Nakazawa, S., Tojo, A., Maruyama, K., Asano, S., 2004. CD19-targeting liposomes containing imatinib efficiently kill Philadelphia chromosome-positive acute lymphoblastic leukemia cells. Blood 104, 1442–1449.

Holmes, R.P., Yeaman, L.D., Taylor, R.G., McCullough, D.L., 1992. Altered neutrophil permeability following shock wave exposure *in vitro*. J. Urol. 147, 733–737.

Kim, S.H., Jeong, J.H., Lee, S.H., Kim, S.W., Park, T.G., 2008. Local and systemic delivery of VEGF siRNA using polyelectrolyte complex micelles for effective treatment of cancer. J. Control. Release 129, 107–116.

Kinoshita, M., Hynynen, K., 2005. A novel method for the intracellular delivery of siRNA using microbubble-enhanced focused ultrasound. Biochem. Biophys. Res. Commun. 335, 393–399.

Kong, X.C., Barzaghi, P., Ruegg, M.A., 2004. Inhibition of synapse assembly in mammalian muscle *in vivo* by RNA interference. EMBO Rep. 5, 183–188.

Lentacker, I., Wang, N., Vandenbroucke, R.E., Demeester, J., De Smedt, S.C., Sanders, N.N., 2009. Ultrasound exposure of lipoplex loaded microbubbles facilitates direct cytoplasmic entry of the lipoplexes. Mol. Pharm. 6, 457–467.

Leong-Poi, H., Christiansen, J., Heppner, P., Lewis, C.W., Klibanov, A.L., Kaul, S., Lindner, J.R., 2005. Assessment of endogenous and therapeutic arteriogenesis by contrast ultrasound molecular imaging of integrin expression. Circulation 111, 3248–3254.

Li, T., Tachibana, K., Kuroki, M., Kuroki, M., 2003. Gene transfer with echo-enhanced contrast agents: comparison between Albunex, Optison, and Levovist in mice—initial results. Radiology 229, 423–428.

Maruyama, K., Ishida, O., Kasaoka, S., Takizawa, T., Utoguchi, N., Shinohara, A., Chiba, M., Kobayashi, H., Eriguchi, M., Yanagie, H., 2004. Intracellular targeting of sodium mercaptoundecahydrododecaborate (BSH) to solid tumors by transferrin-PEG liposomes, for boron neutron-capture therapy (BNCT). J. Control. Release 98, 195–207.

Maruyama, K., Yuda, T., Okamoto, A., Kojima, S., Suginaka, A., Iwatsuru, M., 1992. Prolonged circulation time in vivo of large unilamellar liposomes composed of distearoyl phosphatidylcholine and cholesterol containing amphipathic poly(ethylene glycol). Biochim. Biophys. Acta 1128, 44–49.

McCaffrey, A.P., Meuse, L., Pham, T.T., Conklin, D.S., Hannon, G.J., Kay, M.A., 2002. RNA interference in adult mice. Nature 418, 38–39.

Morrissey, D.V., Lockridge, J.A., Shaw, L., Blanchard, K., Jensen, K., Breen, W., Hartsough, K., Machemer, L., Radka, S., Jadhav, V., Vaish, N., Zinnen, S., Vargeese, C.,

Bowman, K., Shaffer, C.S., Jeffs, L.B., Judge, A., MacLachlan, I., Polisky, B., 2005. Potent and persistent *in vivo* anti-HBV activity of chemically modified siRNAs. Nat. Biotechnol. 23, 1002–1007.

Negishi, Y., Endo-Takahashi, Y., Ishii, K., Suzuki, R., Oguri, Y., Murakami, T., Maruyama, K., Aramaki, Y., 2011a. Development of novel nucleic acid-loaded Bubble liposomes using cholesterol-conjugated siRNA. J. Drug Target 19, 830–836.

Negishi, Y., Endo, Y., Fukuyama, T., Suzuki, R., Takizawa, T., Omata, D., Maruyama, K., Aramaki, Y., 2008. Delivery of siRNA into the cytoplasm by liposomal bubbles and ultrasound. J. Control. Release 132, 124–130.

Negishi, Y., Matsuo, K., Endo-Takahashi, Y., Suzuki, K., Matsuki, Y., Takagi, N., Suzuki, R., Maruyama, K., Aramaki, Y., 2011b. Delivery of an angiogenic gene into ischemic muscle by novel bubble liposomes followed by ultrasound exposure. Pharm. Res. 28, 712–719.

Negishi, Y., Tsunoda, Y., Endo-Takahashi, Y., Oda, Y., Suzuki, R., Maruyama, K., Yamamoto, M., Aramaki, Y., 2011c. Local gene delivery system by bubble liposomes and ultrasound exposure into joint synovium. J. Drug Deliv. 2011, 203986.

Niu, X.Y., Peng, Z.L., Duan, W.Q., Wang, H., Wang, P., 2006. Inhibition of HPV 16 E6 oncogene expression by RNA interference *in vitro* and *in vivo*. Int. J. Gynecol. Cancer 16, 743–751.

Oliveira, S., Fretz, M.M., Høgset, A., Storm, G,, Schiffelers, R.M., 2007. Photochemical internalization enhances silencing of epidermal growth factor receptor through improved endosomal escape of siRNA. Biochim. Biophys. Acta 1768, 1211–1217.

Otani, K., Yamahara, K., Ohnishi, S., Obata, H., Kitamura, S., Nagaya, N., 2009. Nonviral delivery of siRNA into mesenchymal stem cells by a combination of ultrasound and microbubbles. J. Control. Release 133, 146–153.

Palmowski, M., Huppert, J., Ladewig, G., Hauff, P., Reinhardt, M., Mueller, M.M., Woenne, E.C., Jenne, J.W., Maurer, M., Kauffmann, G.W., Semmler, W., Kiessling, F., 2008. Molecular profiling of angiogenesis with targeted ultrasound imaging: early assessment of antiangiogenic therapy effects. Mol. Cancer Ther. 7, 101–109.

Sadzuka, Y., Nakade, A., Hirama, R., Miyagishima, A., Nozawa, Y., Hirota, S., Sonobe, T., 2002. Effects of mixed polyethyleneglycol modification on fixed aqueous layer thickness and antitumor activity of doxorubicin containing liposome. Int. J. Pharm. 238, 171–180.

Sato, Y., Murase, K., Kato, J., Kobune, M., Sato, T., Kawano, Y., Takimoto, R., Takada, K., Miyanishi, K., Matsunaga, T., Takayama, T., Niitsu, Y., 2008. Resolution of liver cirrhosis using vitamin A-coupled liposomes to deliver siRNA against a collagen-specific chaperone. Nat. Biotechnol. 26, 431–442.

Schiffelers, R.M., Xu, J., Storm, G., Woodle, M.C., Scaria, P.V., 2005. Effects of treatment with small interfering RNA on joint inflammation in mice with collagen-induced arthritis. Arthritis Rheum. 52, 1314–1318.

Schratzberger, P., Krainin, J.G., Schratzberger, G., Silver, M., Ma, H., Kearney, M., Zuk, R.F., Brisken, A.F., Losordo, D.W., Isner, J.M., 2002. Transcutaneous ultrasound augments naked DNA transfection of skeletal muscle. Mol. Ther. 6, 576–583.

Song, E., Lee, S.K., Wang, J., Ince, N., Ouyang, N., Min, J., Chen, J., Shankar, P., Lieberman, J., 2003. RNA interference targeting Fas protects mice from fulminant hepatitis. Nat. Med. 9, 347–351.

Sonoda, S., Tachibana, K., Uchino, E., Okubo, A., Yamamoto, M., Sakoda, K., Hisatomi, T., Sonoda, K.H., Negishi, Y., Izumi, Y., Takao, S., Sakamoto, T., 2006. Gene transfer to corneal epithelium and keratocytes mediated by ultrasound with microbubbles. Invest. Ophthalmol. Vis. Sci. 47, 558–564.

Suzuki, J., Ogawa, M., Takayama, K., Taniyama, Y., Morishita, R., Hirata, Y., Nagai, R., Isobe, M., 2010. Ultrasound-microbubble-mediated intercellular adhesion molecule-1 small interfering ribonucleic acid transfection attenuates neointimal formation after arterial injury in mice. J. Am. Coll. Cardiol. 55, 904–913.

Suzuki, R., Takizawa, T., Negishi, Y., Hagisawa, K., Tanaka, K., Sawamura, K., Utoguchi, N., Nishioka, T., Maruyama, K., 2007. Gene delivery by combination of novel liposomal bubbles with perfluoropropane and ultrasound. J. Control. Release 117, 130–136.

Suzuki, R., Takizawa, T., Negishi, Y., Utoguchi, N., Maruyama, K., 2008a. Effective gene delivery with novel liposomal bubbles and ultrasonic destruction technology. Int. J. Pharm. 354, 49–55.

Suzuki, R., Takizawa, T., Negishi, Y., Utoguchi, N., Sawamura, K., Tanaka, K., Namai, E., Oda, Y., Matsumura, Y., Maruyama, K., 2008b. Tumor specific ultrasound enhanced gene transfer *in vivo* with novel liposomal bubbles. J. Control. Release 125, 137–144.

Takei, Y., Nemoto, T., Mu, P., Fujishima, T., Ishimoto, T., Hayakawa, Y., Yuzawa, Y., Matsuo, S., Muramatsu, T., Kadomatsu, K., 2008. *In vivo* silencing of a molecular target by short interfering RNA electroporation: tumor vascularization correlates to delivery efficiency. Mol. Cancer Ther. 7, 211–221.

Takeshita, F., Minakuchi, Y., Nagahara, S., Honma, K., Sasaki, H., Hirai, K., Teratani, T., Namatame, N., Yamamoto, Y., Hanai, K., Kato, T., Sano, A., Ochiya, T., 2005. Efficient delivery of small interfering RNA to bone-metastatic tumors by using atelocollagen *in vivo*. Proc. Natl. Acad. Sci. U.S.A. 102, 12177–12182.

Taniyama, Y., Tachibana, K., Hiraoka, K., Aoki, M., Yamamoto, S., Matsumoto, K., Nakamura, T., Ogihara, T., Kaneda, Y., Morishita, R., 2002a. Development of safe and efficient novel nonviral gene transfer using ultrasound: enhancement of transfection efficiency of naked plasmid DNA in skeletal muscle. Gene Ther. 9, 372–380.

Taniyama, Y., Tachibana, K., Hiraoka, K., Namba, T., Yamasaki, K., Hashiya, N., Aoki, M., Ogihara, T., Yasufumi, K., Morishita, R., 2002b. Local delivery of plasmid DNA into rat carotid artery using ultrasound. Circulation 105, 1233–1239.

Tsunoda, S., Mazda, O., Oda, Y., Iida, Y., Akabame, S., Kishida, T., Shin-Ya, M., Asada, H., Gojo, S., Imanishi, J., Matsubara, H., Yoshikawa, T., 2005. Sonoporation using microbubble BR14 promotes pDNA/siRNA transduction to murine heart. Biochem. Biophys. Res. Commun. 336, 118–127.

Unger, E.C., Porter, T., Culp, W., Labell, R., Matsunaga, T., Zutshi, R., 2004. Therapeutic applications of lipid-coated microbubbles. Adv. Drug Deliv. Rev. 56, 1291–1314.

Vandenbroucke, R.E., Lentacker, I., Demeester, J., De Smedt, S.C., Sanders, N.N., 2008. Ultrasound assisted siRNA delivery using PEG-siPlex loaded microbubbles. J. Control. Release 126, 265–273.

Xia, C.F., Zhang, Y., Zhang, Y., Boado, R.J., Pardridge, W.M., 2007. Intravenous siRNA of brain cancer with receptor targeting and avidin-biotin technology. Pharm. Res. 24, 2309–2316.

International Journal of Pharmaceutics 422 (2012) 332–337

Contents lists available at SciVerse ScienceDirect

International Journal of Pharmaceutics

journal homepage: www.elsevier.com/locate/ijpharm

Note

Gene delivery system involving Bubble liposomes and ultrasound for the efficient *in vivo* delivery of genes into mouse tongue tissue

Marika Sugano[a,b], Yoichi Negishi[b,*], Yoko Endo-Takahashi[b], Ryo Suzuki[c], Kazuo Maruyama[c], Matsuo Yamamoto[a,**], Yukihiko Aramaki[b]

[a] Department of Periodontology, Showa University School of Dentistry, 2-1-1 Kitasenzoku, Ohta-ku, Tokyo 145-8515, Japan
[b] Department of Drug Delivery and Molecular Biopharmaceutics, School of Pharmacy, Tokyo University of Pharmacy and Life Sciences, 1432-1 Horinouchi, Hachioji, Tokyo 192-0392, Japan
[c] Department of Biopharmaceutics, School of Pharmaceutical Sciences, Teikyo University, 1091-1 Suwarashi, Midori-ku, Sagamihara, Kanagawa 252-5195, Japan

ARTICLE INFO

Article history:
Received 16 August 2011
Received in revised form 25 October 2011
Accepted 2 November 2011
Available online 11 November 2011

Keywords:
Bubble liposomes
Ultrasound
Gene delivery
Tongue tissue

ABSTRACT

Oral squamous cell carcinoma is the most common type of head and neck cancer. Recently, efficient, easy, and minimally invasive gene delivery methods are expected to be developed as cancer gene therapies. However, the optimal method for delivering therapeutic genes into oral tissue for cancer treatment has not been elucidated. Therefore, we hypothesized that the tongue is a good target tissue for gene delivery with Bubble liposomes and ultrasound. To assess this, we attempted to deliver a mixture of plasmid DNA encoding a luciferase or enhanced green fluorescent protein, and Bubble liposomes into murine tongue with or without ultrasound exposure. The ultrasound conditions were 1 MHz, 2 W/cm^2, 60 s, and duty cycle: 50%. The time-course of gene expression in the tongue was investigated with a luciferase assay and fluorescent microscopy. Luciferase expression was significantly increased in tongue transfected using Bubble liposomes and ultrasound compared with that of the tongue untreated with ultrasound, and this high level of luciferase activity was maintained for 2 weeks. From these results, Bubble liposomes can be used in combination with ultrasound to efficiently deliver plasmid DNA into the tongue *in vivo*. This technique is a highly promising approach for gene delivery into oral tissue.

© 2011 Elsevier B.V. All rights reserved.

1. Introduction

Although the most common types of oral disease are dental caries and periodontal disease, oral cancer such as squamous cell carcinoma (SCC) is associated with an unfavorable prognosis. Tongue SCC is the most common type of oral SCC, and metastasis to the lymph nodes and/or proximal tissues often occurs (Ohba et al., 2010; Shiga et al., 2007). The current treatments for tongue SCC include surgery, radiation therapy, and chemotherapy, all of which have severe side effects. Therefore, cancer cell-specific treatment that does not damage normal cells is desired. Recently, gene delivery to tumor cells such as using adenovirus-based p53 gene therapies has gained attention (Edelman and Nemunaitis, 2003; Huang et al., 2009). The two main gene carrier systems for gene therapy are viral vectors and non-viral delivery systems. Viral vectors are efficient carriers for gene transfection (Lundstrom, 2003), but some serious problems such as immunogenicity and toxicity have been reported (Check, 2002, 2003; Marshall, 1999). On the other hand, the transfection efficiency of non-viral methods remains a problem. Therefore, it is necessary to develop a safe and highly efficient gene transfer method.

Recently, it has been reported that the use of microbubbles in combination with low energy ultrasound (US) enhances transfection efficiency (Greenleaf et al., 1998; Shohet et al., 2000; Sonoda et al., 2006; Taniyama et al., 2002a,b). Regarding the orofacial area, there have been a few reports about gene delivery using microbubbles and US, for example, Sakai et al. (2009) and Chen et al. (2009) reported transient gene transfection in the target tissue using different microbubbles. However, prolonged gene expression is necessary in the clinical setting, and the size and stability of the microbubbles employed also needs to be improved. Previously, we developed "Bubble liposomes (BL)" as a novel gene delivery carrier system and reported that gene delivery using a combination of BL and US is safer and more efficient in both *in vitro* and *in vivo* compared to other non-viral methods (Negishi et al., 2008, 2011; Suzuki et al., 2007). However, there are no reports about gene delivery to

Abbreviations: SCC, squamous cell carcinoma; US, ultrasound; BL, Bubble liposome; PEG, polyethylene glycol; EBD, Evans blue dye; QOL, quality of life.

* Corresponding author. Tel.: +81 42 676 3183; fax: +81 42 676 3182.
** Corresponding author. Tel: +81 3 5498 1995; fax: +81 3 3787 7886.
E-mail addresses: negishi@toyaku.ac.jp (Y. Negishi), yamamoto-m@dent.showa-u.ac.jp (M. Yamamoto).

0378-5173/$ – see front matter © 2011 Elsevier B.V. All rights reserved.
doi:10.1016/j.ijpharm.2011.11.001

oral tissue using this technique. Therefore, in the present study, we assessed whether efficient gene delivery into mouse tongue tissue could be achieved using BL and US.

2. Materials and methods

2.1. Animals

Five-week-old male ICR mice were used for all animal experiments (Tokyo Laboratory Animals Science, Tokyo, Japan). All studies were approved by the Animal Experiment Committee of Tokyo University of Pharmacy and Life Sciences. The mice were given feed and tap water *ad libitum* throughout the experimental period.

2.2. Preparation of Bubble liposomes

The BL were prepared using the previously described method (Negishi et al., 2008; Suzuki et al., 2007). In brief, PEG liposomes composed of 1,2-dipalmitoyl-sn-glycero-3-phosphocholine (DPPC) (NOF Corporation, Tokyo, Japan) and 1,2-distearoyl-sn-glycero-3-phosphatidyl-ethanolamine-polyethyleneglycol (DSPE-PEG_{2000}-OMe) (NOF Corporation) in a molar ratio of 94:6 were prepared using a reverse phase evaporation method. In brief, all reagents were dissolved in 1:1 (v/v) chloroform/diisopropyl ether. Phosphate-buffered saline was added to the lipid solution, and the mixture was sonicated and then evaporated at 47 °C. Then, the organic solvent was completely removed, and the size of the liposomes was adjusted to less than 200 nm using extruding equipment and a sizing filter (pore size: 200 nm) (Nuclepore Track-Etch Membrane, Whatman plc, UK). The lipid concentration was measured using a Phospholipid C test Wako (Wako Pure Chemical Industries Ltd., Osaka, Japan), and BL were prepared from liposomes and perfluoropropane gas (Takachio Chemical Ind. Co. Ltd., Tokyo, Japan). First, 2-mL sterilized vials containing 0.8 mL of a liposome suspension (lipid concentration: 1 mg/mL) were filled with perfluoropropane gas, capped, and then pressurized with a further 3 mL of perfluoropropane gas. The vial was placed in a bath-type sonicator (42 kHz, 100 W) (Bransonic 2510j-DTH, Branson Ultrasonics Co., Danbury, CT, USA) for 5 min to form BL.

2.3. Plasmid DNA

Two reporter plasmids were used. The pcDNA3-Luc plasmid, which is derived from pGL3-basic (Promega, Madison, WI), is an expression vector encoding the firefly luciferase gene under the control of the cytomegalovirus promoter. The pEGFP-N3 plasmid (Clontech Laboratories, Inc., Mountain View, CA) is an expression vector encoding enhanced green fluorescent protein (EGFP) under the control of the cytomegalovirus promoter.

2.4. In vivo gene delivery using BL and US

ICR mice were anesthetized with 10 mg/mL pentobarbital throughout each procedure. A 20 μL mixture of pDNA (20 μg) and BL (10 μg) was injected into the tongue tissue of the mice using a 33-gauge syringe (Hamilton Company, USA), and US exposure (frequency: 1 MHz; duty: 50%; intensity: 2 W/cm^2; time: 60 s) was immediately applied to the injection site. A Sonitron 2000 (Nepa Gene Co., Ltd.) was used as an ultrasound generator. Several days after the injection, the mice were sacrificed, and the tongue tissue in the US-exposed area was collected and homogenized with Polytron (Kinematica, Inc., New York, USA). The cell lysate and tissue homogenates were prepared with a lysis buffer (0.1 M Tris–HCl (pH 7.8), 0.1% Triton X-100, and 2 mM EDTA). Luciferase activity was then measured using a luciferase assay system (Promega, Madison, WI) and a luminometer (LB96V, Belthold Japan Co. Ltd., Tokyo, Japan). Activity is indicated as relative light units (RLU) per mg of protein. To analyze EGFP expression, the collected tongue was fixed with paraformaldehyde and dehydrated in sucrose solution. The specimens were then embedded in OCT compound and immediately frozen at −80 °C. Serial 10 μm thick sections were then cut using a cryostat and observed with a fluorescence microscope (Axiovert 200 M, Carl Zeiss),

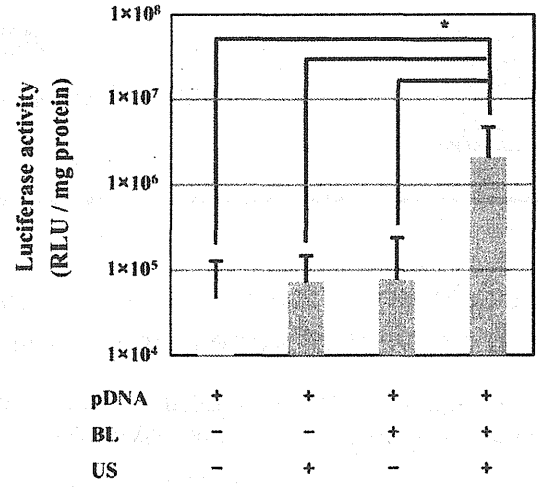

Fig. 1. Luciferase activity in tongue tissue transfected with a reporter gene using BL and US. Mice were subjected to BL and US-mediated luciferase gene transfer. Relative luciferase activity was determined on day 5 after transfection. The data are shown as the mean ± S.D. *$P < 0.05$, Mann–Whitney's U test ($n = 5$), compared to other groups. pDNA (pCMV-luciferase): 20 μg; BL: 10 μg; US conditions: frequency: 1 MHz, duty: 50%, and intensity: 2 W/cm^2, time: 60 s. BL, Bubble liposomes; US, ultrasound.

2.5. Tissue damage testing using Evans blue dye (EBD)

Tissue-damage testing using EBD was performed as reported previously (Liu and Huang, 2002). Briefly, EBD was dissolved in PBS (10 mg/mL) and sterilized using 0.2 μm membrane filters. The mice treated with pDNA, BL, and US were administered EBD (0.5 mg dye/10 g body weight) by tail vein injection and then sacrificed 1 day after the EBD injection. Their tongue tissues were collected, fixed with paraformaldehyde, embedded in OCT compound, and immediately frozen at −80 °C. Serial 10 μm thick sections were cut using a cryostat and observed with a fluorescence microscope (Axiovert 200 M, Carl Zeiss).

2.6. Statistical analysis

All data are shown as the mean ± S.D. ($n = 5$ or 6). Mann–Whitney's U test was used to determine the statistical significance of any differences. The differences detected in multiple comparison tests were assessed by two-way repeated-measures analysis of variance (ANOVA). Differences associated with a $P < 0.05$ were considered significant.

3. Results

We first tried to deliver naked pDNA into tongue tissue using BL and US under the conditions used in a previous study, in which naked pDNA was delivered into skeletal muscles (Negishi et al., 2011). Significantly increased gene expression was detected in the group treated with BL and US exposure (Fig. 1.); i.e., it was 12-fold higher than that of the group treated with pDNA alone. In the groups

treated with pDNA + BL and pDNA + US, the relative luciferase activity remained as low as that of the pDNA alone group.

Then, to optimize the conditions for *in vivo* gene delivery into tongue tissue, we examined three transfection condition parameters, the total pDNA, US intensity, and US exposure time. First, to assess whether the pDNA injection volume affected transfection efficiency, we adjusted it from 0.2 μg to 20 μg. As a result, the increase in luciferase activity was found to be dependent on the amount of pDNA, and the most significant increase in relative luciferase activity was detected at 20 μg pDNA (Fig. 2a.). Next, we investigated the relationship between US intensity and the transfection efficiency of gene delivery into tongue tissue. The US intensity was varied within the 0–4 W/cm^2 range. The relative luciferase activity was significantly higher in the groups treated with US intensities of 2.0 W/cm^2 and 4.0 W/cm^2 (Fig. 2b.). Moreover, we also examined the effect of the US exposure time and found that luciferase activity was highest when US was delivered for 60 s (Fig. 2c.). In contrast, when US was delivered for a longer period, the transfection efficiency tended to decrease. We further examined the duration of gene expression induced after treatment with BL and US exposure. As a result, we found that high luciferase activity was maintained for about 2 weeks (Fig. 3).

Next, the localization of EGFP-expressing cells and tissue damage after gene delivery with BL and US was observed with fluorescence microscopy. In histological observations, distinct EGFP expression was observed in the tongue tissue treated with BL and US (Fig. 4.). In the group treated with BL and US, there were many EGFP expressing cells throughout the muscle layer. In the other groups, only a few sporadically distributed cells were found to express EGFP. However, using a high US intensity to achieve efficient gene transfection leads to tissue damage (Duvshani-Eshet and Machluf, 2005; Kim et al., 1996). Therefore, to investigate the tissue damage caused by gene transfection, mice had EBD injected into their tail veins one day before they were euthanized, as enhanced EBD uptake indicates increased cell damage. As a result, we found that severe tissue damage was observed after the application of high intensity US (4.0 W/cm^2) or a US exposure time of 120 s or more (Fig. 5).

From these results, we suggest that the optimal conditions for gene delivery into the murine tongue using BL and US are as follows: total pDNA (2 μg/μL): 20 μg, US intensity: 2 W/cm^2, and US exposure time: 60 s.

In addition, *Sonazoid*™, a commercially available microbubble, has been used as an echo-contrast gas in clinical. We therefore also test the transfection efficacy of *Sonazoid*™ in the same experiment. However, the luciferase activity was moderate increase even in the combination of US exposure (data not shown).

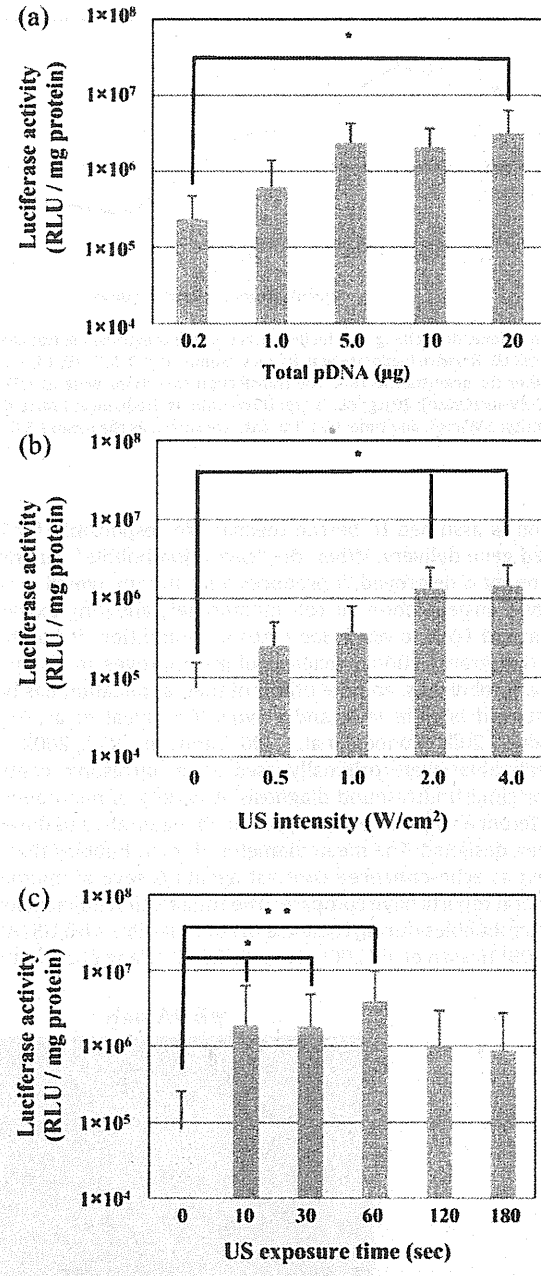

Fig. 2. Characteristics of ultrasound gene delivery systems using BL. To examine the optimal parameters for BL and US-mediated gene transfer into tongue tissue, the mice were subjected to various transfection conditions; i.e., by altering the amount of pDNA, US intensity, and US exposure time. The other conditions were as follows: US frequency: 1 MHz, duty: 50%. The data are shown as the mean ± S.D. (a) The variation in the gene expression level induced by changing the amount of pDNA. The amount of pDNA was changed from 0.2 μg to 20 μg. The total injection volume remained constant at 20 μL. *P < 0.05, Mann–Whitney's U test (n = 5), compared with 0.2 μg of pDNA. (b) The variation in the gene expression level induced by changes in the US intensity. The US intensity was set at 0, 0.5, 1.0, 2.0, or 4.0 W/cm^2. *P < 0.05, Mann–Whitney's U test (n = 5), compared with 0 W/cm^2 (no US exposure). (c) The variation in the gene expression level induced by changes in the US exposure time. The US duration was set at 0, 10, 30, 60, 120, or 180 s. *P < 0.05, **P < 0.01, Mann–Whitney's U test (n = 6), compared with 0 s (no US exposure).

4. Discussion

Gene therapy is expected to be clinically useful for treating genetic diseases, cancer, and/or infectious diseases. These diseases are also found in the orofacial area, and a number of studies have recently examined the usefulness of gene therapy for a variety of oral diseases. In those studies, gene delivery into the orofacial area was performed with viral vectors due to their high transfection efficiency. For example, it has been reported that reporter genes were transfected into rat salivary glands using several kinds of viral vector (Shai et al., 2002; Zheng and Baum, 2005). In addition, viruses are the most common transfer system used to deliver gene therapy to oral SCC (Ladeinde et al., 2005). However, viral systems are not perfect because of their safety and immunogenicity (Check, 2002, 2003; Marshall, 1999).

Therefore, many researchers have tried to establish non-viral gene delivery systems that combine high transfection efficiency with reduced invasiveness. Among these non-viral gene delivery methods, Fechheimer et al. (1987) first reported the US-mediated gene delivery technique, and since then gene transfer using ultrasonic waves has developed into a safe and non-viral gene transfection technology. A physical phenomenon known as

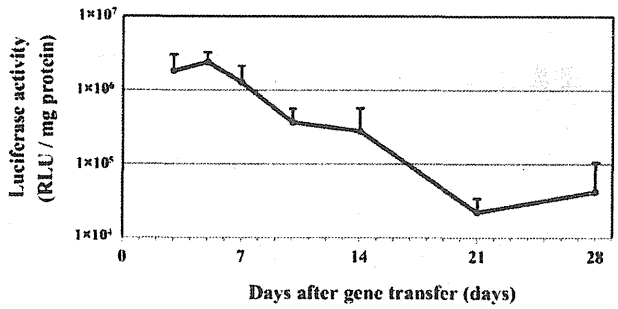

Fig. 3. Time-dependent changes in luciferase activity in tongue tissue transfected using BL and US. Relative luciferase activity was examined at 3, 5, 7, 10, 14, 21, and 28 days after the gene transfection. The transfection conditions were as follows: pDNA (pCMV-luciferase): 20 μg; BL: 10 μg; US conditions: frequency: 1 MHz, duty: 50%, intensity: 2 W/cm^2, and time: 60 s. The data are shown as the mean ± S.D.

cavitation is assumed to be the mechanism responsible for US-mediated gene delivery. When the "cavitation bubble" generated by US energy is destroyed, it produces a jet stream, which in turn produces transient pores in cell membranes, allowing extracellular plasmid DNA to enter the cytosol. In addition, it has been shown that transfection efficiency often improves in the presence of microbubbles, and the utility of their application has been demonstrated both *in vitro* and *in vivo* (Greenleaf et al., 1998; Shohet et al., 2000; Sonoda et al., 2006; Taniyama et al., 2002a,b).

Microbubbles were originally used as an ultrasonic contrast agent for clinical ultrasound diagnosis. A variety of microbubbles with different encapsulated gas types, shell materials, and diluents have been designed. The mean diameter of microbubbles that are marketed as echo-enhanced contrast agents is several micrometers. Several reports have compared the transfection efficiencies of these microbubbles during their use in combination with US (Alter et al., 2009; Hassan et al., 2009; Li et al., 2003; Wang et al., 2005).

However, the intravascular application of microbubbles is hindered by problems with their stability, targeting ability, and particle size. Thus, we developed and applied a new liposome composed of hydrophilic polyethylene glycol (PEG) as a drug delivery system. PEG-liposomes containing perfluoropropane gas are known as "Bubble liposomes (BL)". We have reported that this BL-mediated US gene transfer system enhances transfection efficiency both *in vitro* and *in vivo* (Negishi et al., 2008, 2010; Suzuki et al., 2007, 2008a,b, 2010). Negishi et al. (2011) used gene transfer methods involving BL and US to transfect genes into murine skeletal muscle and discussed their reasons for selecting skeletal muscle as a target tissue for gene therapy. They stated that as skeletal muscle cells are large and display stability and longevity, they are an attractive target tissue for gene therapy.

The generation and oscillation of "cavitation bubbles" after ultrasound exposure is influenced by the composition and pressure of the organs surrounding the transfection site. Therefore, it is important to optimize each transfection condition in the targeted tissue. The majority of tongue tissue is composed of skeletal muscle and is covered with a keratinized oral mucosa. In our histological observations, distinct EGFP expression was observed in the tongue muscle, as shown in Fig. 4. On the other hand, scattered EGFP expression was observed on the surface area of the mucoepithelial layer (data not shown). Moreover, a previous report described that repeated US exposure enhances transfection efficiency and prolonged gene expression compared with single US exposure (Bekeredjian et al., 2003). In this study, we showed that high luciferase activity was maintained for 2 weeks in murine tongue tissue treated with BL and single US exposure. Such persistent expression is thought to be suitable for therapy against tongue cancer. Whether the effect of the therapeutic gene needs to be continuous depends on the disease being targeted; for example, whether it is an infectious or genetic disease. Therefore, if the gene delivery method involving BL and US is to be applied to other oral tissues, it is very important to optimize the transfection conditions for long-term gene expression in the target tissue. Further

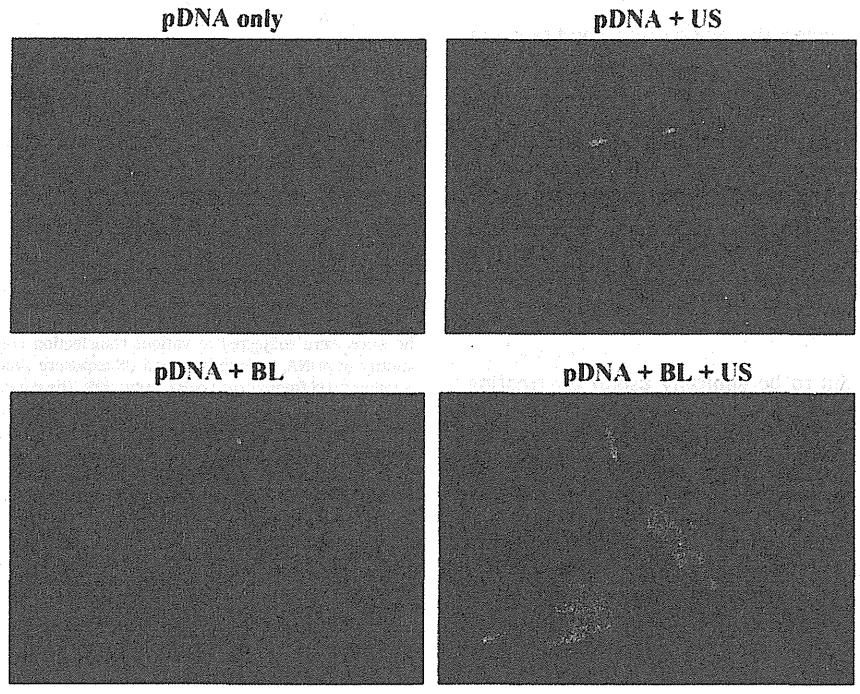

Fig. 4. EGFP expression in tongue tissue transfected with a reporter gene using BL and US. Mice were treated with BL and then subjected to US-mediated EGFP transfer into the tongue. On day 5 after the transfection, the tongue was sectioned into 10 μm thick slices using a cryostat, and EGFP expression was analyzed by fluorescent microscopy. Each of the gene transfer conditions is indicated above the pictures. Magnification: 200×. BL, Bubble liposomes; US, ultrasound.

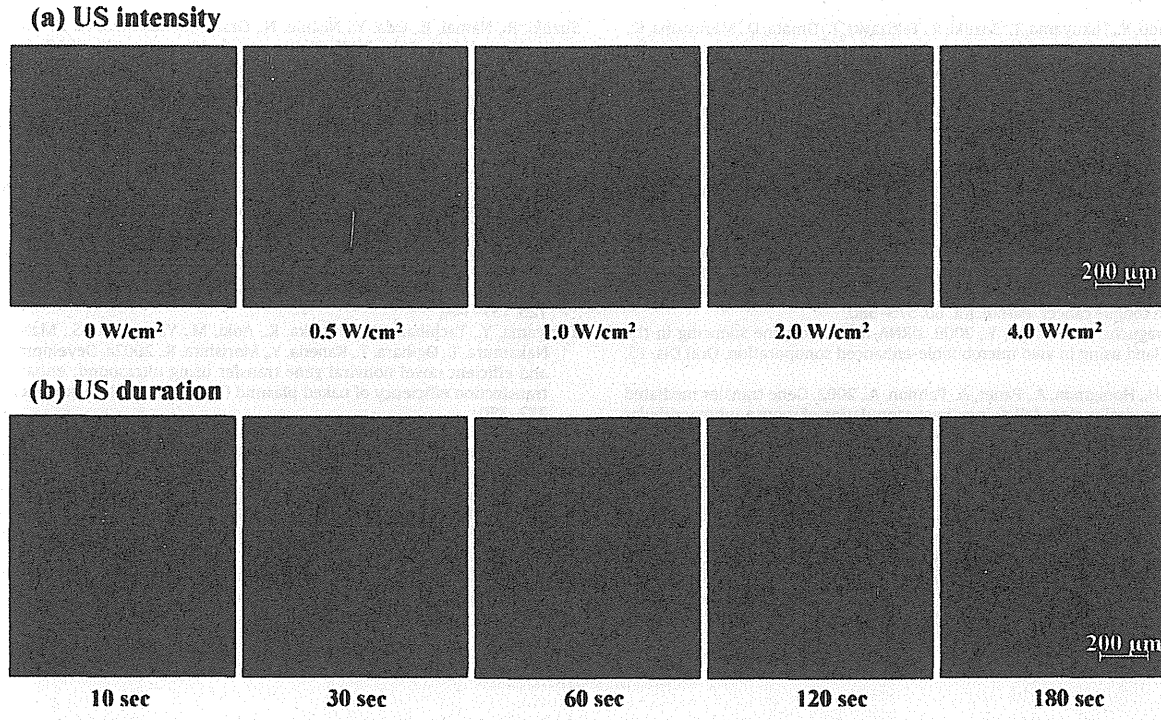

Fig. 5. Tissue-damage testing using EBD. To assess the tissue-damage by BL and US-mediated gene transfer into tongue tissue, the mice were treated pDNA with BL and various US exposure conditions. (a) At a frequency of 1 MHz with an intensity of 0, 0.5, 1.0, 2.0, or 4.0 W/cm^2 for 60 s (upper section). (b) At a frequency of 1 MHz with an intensity of 2.0 W/cm^2 for 10, 30, 60, 120, or 180 s (lower). Evans-blue fluorescence of 10 μm cryosections from the tongue was examined with fluorescence microscopy. Scale bar: 200 μm.

experiments using genes that encode therapeutic proteins are required to assess the clinical application of this US-mediated BL method.

This is the first report regarding gene transfer to tongue tissue using BL and US as a therapeutic method for diseases of the oral cavity. As mentioned above, tongue SCC is one of the most common forms of head and neck cancer; nevertheless, no standardized treatment strategy for this condition has been established (Shiga et al., 2007). Oral dysfunction and decreased quality of life (QOL) are often seen after surgical treatment in tongue SCC patients. Therefore, gene delivery systems involving BL and US exposure that enable cancer cell-specific treatment may improve the QOL of tongue SCC patients.

5. Conclusion

In conclusion, the results of this study suggest that our gene delivery method involving BL and US could be a useful treatment for patients with tongue SCC. This US-mediated BL technique is a highly promising approach for gene delivery into oral tissue.

Acknowledgements

We are grateful to Dr. Katsuro Tachibana (Department of Anatomy, School of Medicine, Fukuoka University) for technical advice regarding the induction of cavitation with US, and to Mr. Yasuhiko Hayakawa and Mr. Kosho Suzuki (Nepa Gene Co., Ltd.) for technical advice regarding US exposure. This study was supported in part by the Industrial Technology Research Grant Program (04A05010) from New Energy, the Industrial Technology Development Organization (NEDO) of Japan.

References

Alter, J., Sennoga, C.A., Lopes, D.M., Eckersley, R.J., Wells, D.J., 2009. Microbubble stability is a major determinant of the efficiency of ultrasound and microbubble mediated in vivo gene transfer. Ultrasound Med. Biol. 35, 976–984.
Bekeredjian, R., Chen, S., Frenkel, P.A., Grayburn, P.A., Shohet, R.V., 2003. Ultrasound-targeted microbubble destruction can repeatedly direct highly specific plasmid expression to the heart. Circulation 108, 1022–1026.
Check, E., 2002. Safety panel backs principle of gene-therapy trials. Nature 420, 595.
Check, E., 2003. Second cancer case halts gene-therapy trials. Nature 421, 305.
Chen, R., Chiba, M., Mori, S., Fukumoto, M., Kodama, T., 2009. Periodontal gene transfer by ultrasound and nano/microbubbles. J. Dent. Res. 88, 1008–1013.
Duvshani-Eshet, M., Machluf, M., 2005. Therapeutic ultrasound optimization for gene delivery: a key factor achieving nuclear DNA localization. J. Control. Release 108, 513–528.
Edelman, J., Nemunaitis, J., 2003. Adenoviral p53 gene therapy in squamous cell cancer of the head and neck region. Curr. Opin. Mol. Ther. 5, 611–617.
Fechheimer, M., Boylan, J.F., Parker, S., Sisken, J.E., Patel, G.L., Zimmer, S.G., 1987. Transfection of mammalian cells with plasmid DNA by scrape loading and sonication loading. Proc. Natl. Acad. Sci. U.S.A. 84, 8463–8467.
Greenleaf, W.J., Bolander, M.E., Sarkar, G., Goldring, M.B., Greenleaf, J.F., 1998. Artificial cavitation nuclei significantly enhance acoustically induced cell transfection. Ultrasound Med. Biol. 24, 587–595.
Hassan, M.A., Feril Jr., L.B., Suzuki, K., Kudo, N., Tachibana, K., Kondo, T., 2009. Evaluation and comparison of three novel microbubbles: enhancement of ultrasound-induced cell death and free radicals production. Ultrason. Sonochem. 16, 372–378.
Huang, P.I., Chang, J.F., Kirn, D.H., Liu, T.C., 2009. Targeted genetic and viral therapy for advanced head and neck cancers. Drug Discov. Today 14, 570–578.
Kim, H.J., Greenleaf, J.F., Kinnick, R.R., Bronk, J.T., Bolander, M.E., 1996. Ultrasound-mediated transfection of mammalian cells. Hum. Gene Ther. 7, 1339–1346.
Ladeinde, A.L., Ogunlewe, M.O., Adeyemo, W.L., Bamgbose, B.O., 2005. Gene therapy in the management of oral cancer: a review of recent developments. Niger. Postgrad. Med. J. 12, 18–22.
Li, T., Tachibana, K., Kuroki, M., 2003. Gene transfer with echo-enhanced contrast agents: comparison between Albunex, Optison, and Levovist in mice – initial results. Radiology 229, 423–428.
Liu, F., Huang, L., 2002. A syringe electrode device for simultaneous injection of DNA and electrotransfer. Mol. Ther. 5, 323–328.
Lundstrom, K., 2003. Latest development in viral vectors for gene therapy. Trends Biotechnol. 21, 117–122.
Marshall, E., 1999. Gene therapy death prompts review of adenovirus vector. Science 286, 2244–2245.

Negishi, Y., Endo, Y., Fukuyama, T., Suzuki, R., Takizawa, T., Omata, D., Maruyama, K., Aramaki, Y., 2008. Delivery of siRNA into the cytoplasm by liposomal bubbles and ultrasound. J. Control. Release 132, 124–130.

Negishi, Y., Matsuo, K., Endo-Takahashi, Y., Suzuki, K., Matsuki, Y., Takagi, N., Suzuki, R., Maruyama, K., Aramaki, Y., 2011. Delivery of an angiogenic gene into ischemic muscle by novel Bubble liposomes followed by ultrasound exposure. Pharm. Res. 28, 712–719.

Negishi, Y., Omata, D., Iijima, H., Takabayashi, Y., Suzuki, K., Endo, Y., Suzuki, R., Maruyama, K., Nomizu, M., Aramaki, Y., 2010. Enhanced laminin-derived peptide AG73-mediated liposomal gene transfer by Bubble liposomes and ultrasound. Mol. Pharmacol. 7, 217–226.

Ohba, T., Motoi, N., Kimura, Y., Okumura, S., Kawabata, K., Yoshizawa, Y., Inase, N., Ishikawa, Y., 2010. Cytokeratin expression profiling is useful for distinguishing between primary squamous cell carcinoma of the lung and pulmonary metastases from tongue cancer. Pathol. Int. 60, 575–580.

Sakai, T., Kawaguchi, M., Kosuge, Y., 2009. siRNA-mediated gene silencing in the salivary gland using in vivo microbubble-enhanced sonoporation. Oral Dis. 15, 505–511.

Shai, E., Falk, H., Honigman, A., Panet, A., Palmon, A., 2002. Gene transfer mediated by different viral vectors following direct cannulation of mouse submandibular salivary glands. Eur. J. Oral Sci. 110, 254–260.

Shiga, K., Ogawa, T., Sagai, S., Kato, K., Kobayashi, T., 2007. Management of the patients with early stage oral tongue cancers. Tohoku J. Exp. Med. 212, 389–396.

Shohet, R.V., Chen, S., Zhou, Y.T., Wang, Z., Meidell, R.S., Unger, R.H., Grayburn, P.A., 2000. Echocardiographic destruction of albumin microbubbles directs gene delivery to the myocardium. Circulation 101, 2554–2556.

Sonoda, S., Tachibana, K., Uchino, E., Okubo, A., Yamamoto, M., Sakoda, K., Hisatomi, T., Sonoda, K.H., Negishi, Y., Izumi, Y., Takao, S., Sakamoto, T., 2006. Gene transfer to corneal epithelium and keratocytes mediated by ultrasound with microbubbles. Invest. Ophthalmol. Vis. Sci. 47, 558–564.

Suzuki, R., Namai, E., Oda, Y., Nishiie, N., Otake, S., Koshima, R., Hirata, K., Taira, Y., Utoguchi, N., Negishi, Y., Nakagawa, S., Maruyama, K., 2010. Cancer gene therapy by IL-12 gene delivery using liposomal bubbles and tumoral ultrasound exposure. J. Control. Release 142, 245–250.

Suzuki, R., Takizawa, T., Negishi, Y., Hagisawa, K., Tanaka, K., Sawamura, K., Utoguchi, N., Nishioka, T., Maruyama, K., 2007. Gene delivery by combination of novel liposomal bubbles with perfluoropropane and ultrasound. J. Control. Release 117, 130–136.

Suzuki, R., Takizawa, T., Negishi, Y., Utoguchi, N., Maruyama, K., 2008a. Effective gene delivery with novel liposomal bubbles and ultrasonic destruction technology. Int. J. Pharm. 354, 49–55.

Suzuki, R., Takizawa, T., Negishi, Y., Utoguchi, N., Sawamura, K., Tanaka, K., Namai, E., Oda, Y., Matsumura, Y., Maruyama, K., 2008b. Tumor specific ultrasound enhanced gene transfer in vivo with novel liposomal bubbles. J. Control. Release 125, 137–144.

Taniyama, Y., Tachibana, K., Hiraoka, K., Aoki, M., Yamamoto, S., Matsumoto, K., Nakamura, T., Ogihara, T., Kaneda, Y., Morishita, R., 2002a. Development of safe and efficient novel nonviral gene transfer using ultrasound: enhancement of transfection efficiency of naked plasmid DNA in skeletal muscle. Gene Ther. 9, 372–380.

Taniyama, Y., Tachibana, K., Hiraoka, K., Namba, T., Yamasaki, K., Hashiya, N., Aoki, M., Ogihara, T., Yasufumi, K., Morishita, R., 2002b. Local delivery of plasmid DNA into rat carotid artery using ultrasound. Circulation 105, 1233–1239.

Wang, X., Liang, H.D., Dong, B., Lu, Q.L., Blomley, M.J., 2005. Gene transfer with microbubble ultrasound and plasmid DNA into skeletal muscle of mice: comparison between commercially available microbubble contrast agents. Radiology 237, 224–229.

Zheng, C., Baum, B.J., 2005. Evaluation of viral and mammalian promoters for use in gene delivery to salivary glands. Mol. Ther. 12, 528–536.